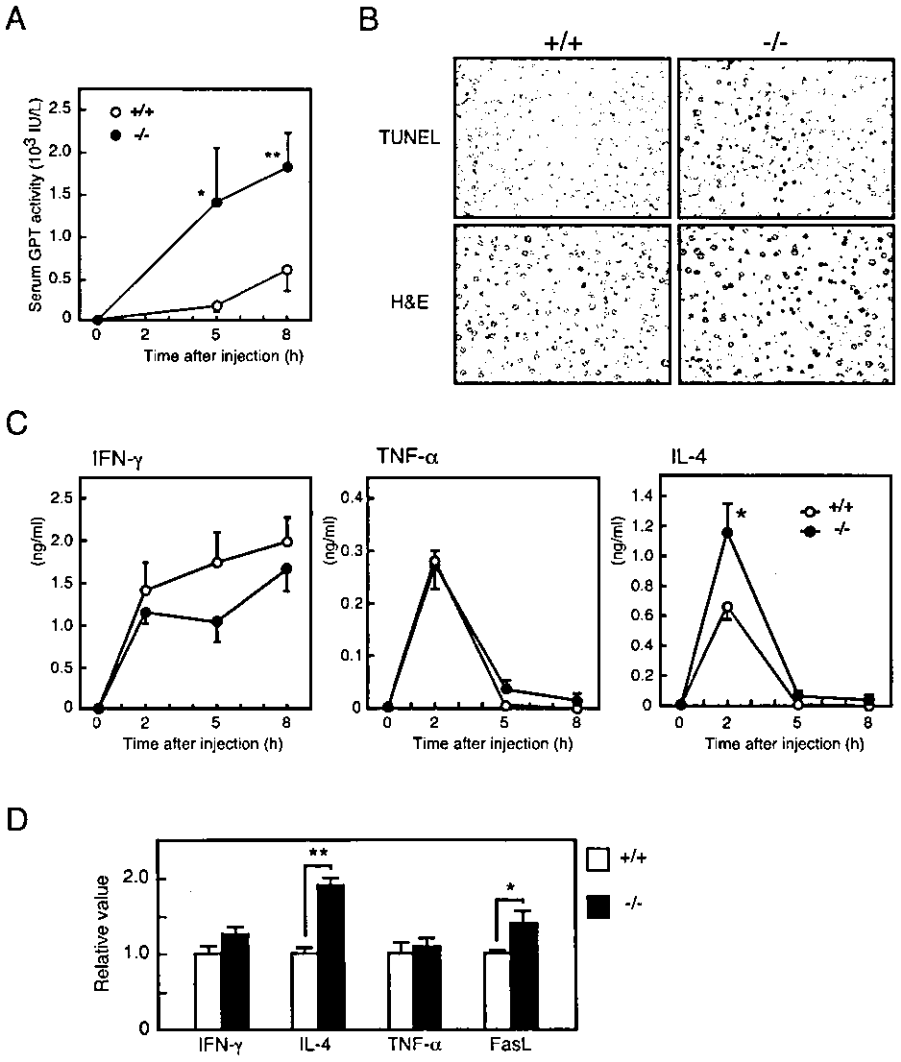

FIGURE 5. Con A-induced hepatitis. *A*, Serum GPT levels (mean ± SD) of wild-type (○) and LECT2$^{-/-}$ (●) mice were measured as described in *Materials and Methods* (n = 8 at each time point). *, $p < 0.05$; **, $p < 0.01$. *B*, Mice treated with Con A were killed at 5 h, and livers were processed for histological analysis. In situ TUNEL staining of liver sections was performed to identify apoptotic cells. *C*, Changes of serum IFN-γ, TNF-α, and IL-4 levels (mean ± SD) in Con A-induced hepatitis. The serum concentrations of cytokines from wild-type (○) and LECT2$^{-/-}$ (●) mice were measured as described above (n = 8 at each time point). *, $p < 0.05$. *D*, Quantitative real-time RT-PCR analysis for cytokine expression. Total liver RNAs were prepared from mice 2 h after Con A injection. The relative ratios of PCR products detected in wild-type mice (assigned a value of 1) vs LECT2$^{-/-}$ mice are indicated (n = 5). *, $p < 0.05$; **, $p < 0.01$.

cytokine levels during the course of the liver injury. Significant elevation of IL-4 in the serum was observed in LECT2$^{-/-}$ mice (Fig. 5*C*). In contrast, the levels of TNF-α and IFN-γ were not significantly different between wild-type and LECT2$^{-/-}$ mice (Fig. 5*C*). Furthermore, the levels of IL-6 and IL-10 in these mouse types were also comparable (data not shown). To compare the local expression of cytokines, quantitative real-time RT-PCR analysis of liver tissue RNA at 2 h after Con A injection was performed. The results revealed that IL-4 and FasL expression in the liver of LECT2$^{-/-}$ mice was significantly higher than that in wild-type liver (Fig. 5*D*). FasL is known as an effector molecule in Con A-induced hepatic injury, and NKT cells primarily express it (16). Thus, the increased hepatic LECT2$^{-/-}$ NKT cells contribute to the severity of Con A-induced hepatitis.

FasL expression and increase in annexin V-positive CD3^{int} NK1.1$^+$ cells during Con A-induced hepatitis

To examine whether the NKT cells of LECT2$^{-/-}$ mice indeed expressed large amounts of FasL upon stimulation with Con A, the proportion of CD3^{int} NK1.1$^+$ cells expressing FasL was determined by flow cytometric analysis. Three hours after Con A injection, the CD3^{int} NK1.1$^+$ cells in LECT2$^{-/-}$ mice expressed approximately twice the amount of FasL that was found in wild-type mice (Fig. 6*A*). Conventional T cells of both wild-type and LECT2$^{-/-}$ mice expressed scarcely any FasL (Fig. 6*A*).

Next, we analyzed the proportion of NKT cells that become apoptotic upon stimulation with Con A, because current evidence suggests that hepatic NKT cells are eliminated by apoptosis after Con A injection (16). The three-color staining of CD3^{int} NK1.1$^+$ and annexin-V demonstrated that hepatic CD3^{int} NK1.1$^+$ cells of both wild-type and LECT2$^{-/-}$ mice decreased 3 h after Con A injection, and the proportion of annexin V-positive cells was higher in LECT2$^{-/-}$ mice. In contrast, conventional T cells were not stained with annexin V (Fig. 6*B*). These results suggest that hepatic NKT cells in LECT2$^{-/-}$ mice showed increased activation-dependent apoptosis, as is the case in wild-type mice.

Discussion

LECT2 was originally noted for its possible neutrophil chemotactic activity (1). In addition, it was independently reported to be a growth-stimulating factor for chondrocytes and osteoblasts and was named chondromodulin II (6). To determine the function of LECT2 in vivo, we generated LECT2$^{-/-}$ mice. In some preliminary experiments we could not easily find any clear differences related to the above two activities. Therefore, based on the possible roles of LECT2 in liver injury and its tissue-specific expression (2, 3), we focused on the liver.

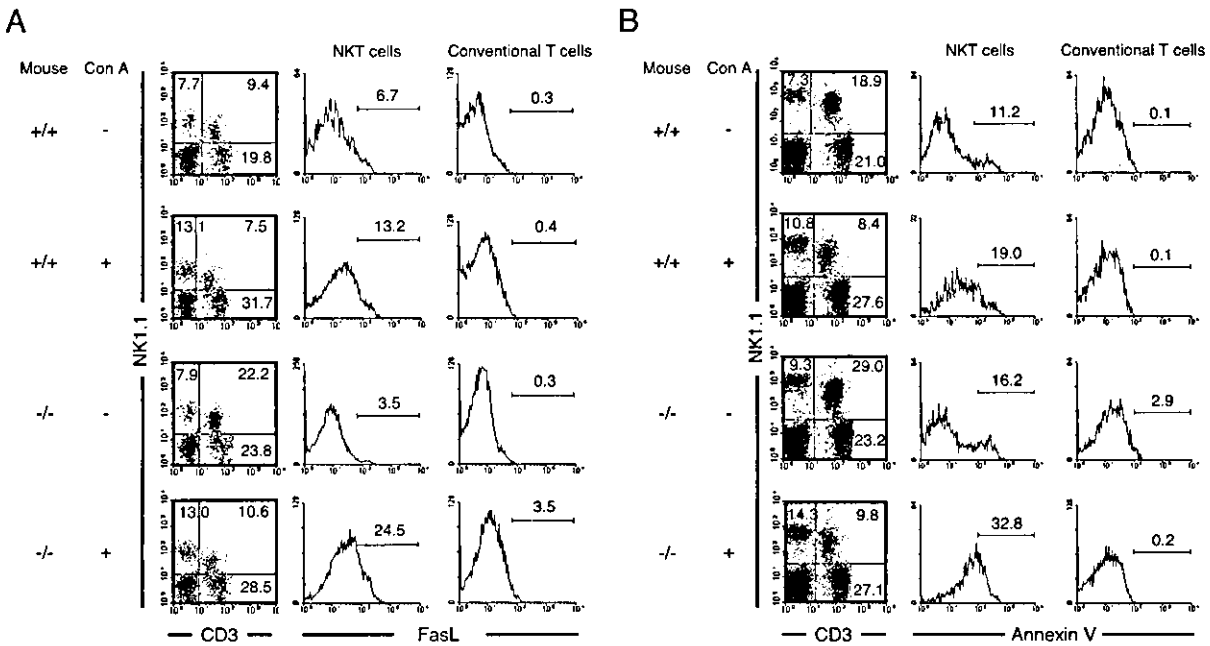

FIGURE 6. Detections of NKT cells expressing FasL or annexin V-positive NKT cells during Con A-induced hepatitis. *A*, NKT cells or conventional T cells that express FasL were detected by three-color staining for CD3, NK1.1, and FasL. Hepatic MNCs were prepared 3 h after injection with Con A or control saline. *B*, Increase in annexin V-positive NKT cells in the livers of mice challenged with Con A. Hepatic MNCs were isolated 3 h after the Con A challenge. Three-color staining was performed for CD3, NK1.1, and annexin V.

In the present study we found an increased proportion of hepatic CD3^{int} NK1.1$^+$ and CD4$^+$ NK1.1$^+$ cells in LECT2$^{-/-}$ mice compared with that in wild-type mice (Fig. 2*A*). Moreover, we observed that the proportion of hepatic CD3^{int} CD1d-α-GalCer tetramer$^+$ cells in LECT2$^{-/-}$ mice was about double that in wild-type mice (Fig. 2*C*), indicating that LECT2$^{-/-}$ mice have an increased proportion of hepatic Vα14 NKT cells. The production of IL-4 and IFN-γ 2 h after administration of α-GalCer in mice would be primarily derived from NKT cells (30). Furthermore, the higher production of both cytokines from the hepatic MNCs treated with α-GalCer is consistent with this result. Therefore, the differences in the levels of IL-4 and IFN-γ after stimulation with α-GalCer in vivo and in vitro could be explained by the increased number of NKT cells in LECT2$^{-/-}$ mice. In addition, the Fas/FasL-sensitive cytotoxicity of hepatic MNCs in LECT2$^{-/-}$ mice was much higher than that in wild-type mice. In contrast, this cytotoxicity of spleen cells from both wild-type and LECT2$^{-/-}$ mice was comparable. We also could find no significant differences in the percentage of CD3^{int} NK1.1$^+$ cells in the spleen cells of LECT2$^{-/-}$ and wild-type mice. Therefore, augmentation of the Fas/FasL-sensitive cytotoxicity shown in hepatic MNCs was possibly due to the increased percentage of NKT cells in LECT2$^{-/-}$ mice. In addition, the NK-sensitive cytotoxicity in hepatic MNCs from LECT2$^{-/-}$ mice was slightly higher than that in MNCs from wild-type mice. At present, although the reason for this slight enhancement is not clear, the cytotoxicity of hepatic NK cells also might be enhanced in LECT2$^{-/-}$ mice. Thus, all these results indicate that LECT2$^{-/-}$ mice show an increase in hepatic NKT cells, which appear to function as they do in wild-type mice.

To explore the biological effects of the increased number of hepatic NKT cells in LECT2$^{-/-}$ mice, we compared wild-type and LECT2$^{-/-}$ mice using the Con A-induced hepatitis model. The onset of Con A-induced hepatitis requires a complicated process of activation of cytokines from immune cells. Both IFN-γ and TNF-α play crucial roles in Con A-induced hepatitis (29, 31). Recent reports have pointed out that activated NKT cells expressing IL-4 also play an essential role in Con A-induced hepatitis and mediate subsequent activation of the cytotoxic pathways (14–16). We showed that LECT2$^{-/-}$ mice were clearly sensitive to Con A-induced hepatitis (Fig. 5, *A* and *B*), and that the levels of IL-4 and FasL in LECT2$^{-/-}$ mice were higher than those in wild-type mice (Fig. 5, *C* and *D*). These findings strongly suggest that a higher level of IL-4 expression induces excessive FasL and also probably granzyme B (15), resulting in the production of a number of apoptotic hepatocytes (Fig. 5*B*) and a larger proportion of annexin V-positive hepatic CD3^{int} NK1.1$^+$ cells (Fig. 6). Recently, several reports showed that the NK1.1 marker of CD3^{int} NK1.1$^+$ cells is down-modulated on activation (32–35). Therefore, the decrease in CD3^{int} NK1.1$^+$ cells after Con A challenge in both wild-type and LECT2$^{-/-}$ mice (Fig. 6) might be due not only to apoptosis of NKT cells, but also to down-regulation of the NK1.1 marker.

The reason for the increase in hepatic NKT cells in LECT2$^{-/-}$ mice is an important issue. LECT2 might participate in the differentiation, development, or both of NKT cell lineages. There is considerable evidence for genes that positively regulate the development of NK or NKT lineages (36). In contrast, LECT2$^{-/-}$ mice have an increase in NKT cells in the liver, suggesting that LECT2 might negatively regulate the development of NKT cell lineages. However, considering that there were no obvious differences in CD3^{int} NK1.1$^+$ cells of spleen, thymus, and bone marrow (Fig. 2*C*; data not shown), a role for LECT2 might be related to the homeostasis of NKT cells in the liver. For example, LECT2 might control an immune state in the liver by regulating the selection and/or expansion of hepatic NKT cells or the homing activity of NKT cells toward the liver. Moreover, a distinctive feature of NKT cells in LECT2$^{-/-}$ mice is that the difference in IL-4 production between wild-type and LECT2$^{-/-}$ mice is greater than that in IFN-γ production upon stimulation with α-GalCer. The possible IL-4 dominance might be related to the observation that mice containing an increased number of NKT cells tend to be IL-4 dominant (37–40), or immature NKT cell lineages tend to exhibit the

Th2-type-dominant phenotype (41, 42). It is possible that an imbalance in the proportion of NKT cells in LECT2$^{-/-}$ mice affects an immune state, which is associated with the pathogenesis of certain immune diseases.

In summary, our results revealed that the number of hepatic NKT cells was increased in LECT2$^{-/-}$ mice and suggested that LECT2 may play an important role in the homeostasis of NKT cells in the liver. Although a deficiency of LECT2 does not cause any significant abnormality in mice under physiological conditions, they become susceptible to Con A-induced hepatitis, probably due to excessive production of IL-4 and FasL from NKT cells. Thus, it is possible that LECT2 might be involved in the pathogenesis of hepatitis or other inflammatory diseases in humans through modulation of NKT cell activity.

Acknowledgments

We kindly thank Dr. Yasuhiko Koezuka (Kirin Brewery, Pharmaceutical Research Laboratory) for useful comments.

References

1. Yamagoe, S., Y. Yamakawa, Y. Matsuo, J. Minowada, S. Mizuno, and K. Suzuki. 1996. Purification and primary amino acid sequence of a novel neutrophil chemotactic factor LECT2. *Immunol. Lett. 52:9.*
2. Yamagoe, S., S. Mizuno, and K. Suzuki. 1998. Molecular cloning of human and bovine LECT2 having a neutrophil chemotactic activity and its specific expression in the liver. *Biochim. Biophys. Acta 1396:105.*
3. Segawa, Y., Y. Itokazu, N. Inoue, T. Saito, and K. Suzuki. 2001. Possible changes in expression of chemotaxin LECT2 mRNA in mouse liver after concanavalin A-induced hepatic injury. *Biol. Pharm. Bull. 24:425.*
4. Ness, S. A., Å. Marknell, and T. Graf. 1989. The v-*myb* oncogene product binds to and activates the promyelocyte-specific *mim-1* gene. *Cell 59:1115.*
5. Fujiki, K., D.-H. Shin, M. Nakao, and T. Yano. 2000. Molecular cloning of carp (*Cyprinus carpio*) leucocyte cell-derived chemotaxin 2, glia maturation factor β, CD45 and lysozyme C by use of suppression subtractive hybridization. *Fish Shellfish Immunol. 10:643.*
6. Hiraki, Y., H. Inoue, J. Kondo, A. Kamizono, Y. Yoshitake, C. Shukunami, and F. Suzuki. 1996. A novel growth-promoting factor derived from fetal bovine cartilage, chondromodulin. II. Purification and amino acid sequence. *J. Biol. Chem. 271:22657.*
7. Kameoka, Y., S. Yamagoe, Y. Hatano, T. Kasama, and K. Suzuki. 2000. Val^{58}Ile polymorphism of the neutrophil chemoattractant *LECT2* and rheumatoid arthritis in the Japanese population. *Arthritis Rheum. 43:1419.*
8. Tiegs, G., J. Hentschel, and A. Wendel. 1992. A T cell-dependent experimental liver injury in mice inducible by concanavalin A. *J. Clin. Invest. 90:196.*
9. Bendelac, A. 1995. Mouse NK$^+$ T cells. *Curr. Opin. Immunol. 7:367.*
10. Bendelac, A., M. N. Rivera, S.-H. Park, and J. H. Roark. 1997. Mouse CD1-specific NK1 T cells: development, specificity, and function. *Annu. Rev. Immunol. 15:535.*
11. MacDonald, H. R. 1995. NK1.1$^+$ T cell receptor-α/β^+ cells: new clues to their origin, specificity, and function. *J. Exp. Med. 182:633.*
12. Godfrey, D. I., K. J. Hammond, L. D. Poulton, M. J. Smyth, and A. G. Baxter. 2000. NKT cells: facts, functions and fallacies. *Immunol. Today 21:573.*
13. Abo, T., T. Kawamura, and H. Watanabe. 2000. Physiological responses of extrathymic T cells in the liver. *Immunol. Rev. 174:135.*
14. Toyabe, S., S. Seki, T. Iiai, K. Takeda, K. Shirai, H. Watanabe, H. Hiraide, M. Uchiyama, and T. Abo. 1997. Requirement of IL-4 and liver NK1$^+$ T cells for concanavalin A-induced hepatic injury in mice. *J. Immunol. 159:1537.*
15. Kaneko, Y., M. Harada, T. Kawano, M. Yamashita, Y. Shibata, F. Gejyo, T. Nakayama, and M. Taniguchi. 2000. Augmentation of Vα14 NKT cell-mediated cytotoxicity by interleukin 4 in an autocrine mechanism resulting in the development of concanavalin A-induced hepatitis. *J. Exp. Med. 191:105.*
16. Takeda, K., Y. Hayakawa, L. van Kaer, H. Matsuda, H. Yagita, and K. Okumura. 2000. Critical contribution of liver natural killer T cells to a murine model of hepatitis. *Proc. Natl. Acad. Sci. USA 97:5498.*
17. Yamagoe, S., T. Watanabe, S. Mizuno, and K. Suzuki. 1998. The mouse *Lect2* gene: cloning of cDNA and genomic DNA, structural characterization and chromosomal localization. *Gene 216:171.*
18. Soriano, P., C. Montgomery, R. Geske, and A. Bradley. 1991. Targeted disruption of the *c-src* proto-oncogene leads to osteopetrosis in mice. *Cell 64:693.*
19. Horai, R., M. Asano, K. Sudo, H. Kanuka, M. Suzuki, M. Nishihara, M. Takahashi, and Y. Iwakura. 1998. Production of mice deficient in genes for interleukin (IL)-1α, IL-1β, IL-1α/β, and IL-1 receptor antagonist shows that IL-1β is crucial in turpentine-induced fever development and glucocorticoid secretion. *J. Exp. Med. 187:1463.*
20. Watanabe, H., K. Ohtsuka, M. Kimura, Y. Ikarashi, K. Ohmori, A. Kusumi, T. Ohteki, S. Seki, and T. Abo. 1992. Details of an isolation method for hepatic lymphocytes in mice. *J. Immunol. Methods 146:145.*
21. Stanic, A. K., A. D. De Silva, J.-J. Park, V. Sriram, S. Ichikawa, Y. Hirabayashi, K. Hayakawa, L. van Kaer, R. R. Brutkiewicz, and S. Joyce. 2003. Defective presentation of the CD1d1-restricted natural Va14Ja18 NKT lymphocyte antigen caused by β-D-glucosylceramide synthase deficiency. *Proc. Natl. Acad. Sci. USA 100:1849.*
22. Moroda, T., T. Iiai, S. Suzuki, A. Tsukahara, T. Tada, M. Nose, K. Hatakeyama, S. Seki, K. Takeda, H. Watanabe, et al. 1997. Autologous killing by a population of intermediate T-cell receptor cells and its NK1.1$^+$ and NK1.1$^-$ subsets, using Fas ligand/Fas molecules. *Immunology 91:219.*
23. Benlagha, K., A. Weiss, A. Beavis, L. Teyton, and A. Bendelac. 2000. In vivo identification of glycolipid antigen-specific T cells using fluorescent CD1d tetramers. *J. Exp. Med. 191:1895.*
24. Matsuda, J. L., O. V. Naidenko, L. Gapin, T. Nakayama, M. Taniguchi, C.-R. Wang, Y. Koezuka, and M. Kronenberg. 2000. Tracking the response of natural killer T cells to a glycolipid antigen using CD1d tetramers. *J. Exp. Med. 192:741.*
25. Kawano, T., J. Cui, Y. Koezuka, I. Toura, Y. Kaneko, K. Motoki, H. Ueno, R. Nakagawa, H. Sato, E. Kondo, et al. 1997. CD1d-restricted and TCR-mediated activation of Vα14 NKT cells by glycosylceramides. *Science 278:1626.*
26. Osman, Y., T. Kawamura, T. Naito, K. Takeda, L. van Kaer, K. Okumura, and T. Abo. 2000. Activation of hepatic NKT cells and subsequent liver injury following administration of α-galactosylceramide. *Eur. J. Immunol. 30:1919.*
27. Miyaji, C., H. Watanabe, R. Miyakawa, H. Yokoyama, C. Tsukada, Y. Ishimoto, S. Miyazawa, and T. Abo. 2002. Identification of effector cells for TNFα-mediated cytotoxicity against WEHI164S cells. *Cell. Immunol. 216:43.*
28. Hayakawa, Y., K. Takeda, H. Yagita, S. Kakuta, Y. Iwakura, L. van Kaer, I. Saiki, and K. Okumura. 2001. Critical contribution of IFN-γ and NK cells, but not perforin-mediated cytotoxicity, to anti-metastatic effect of α-galactosylceramide. *Eur. J. Immunol. 31:1720.*
29. Mizuhara, H., E. O'Neill, N. Seki, T. Ogawa, C. Kusunoki, K. Otsuka, S. Satoh, M. Niwa, H. Senoh, and H. Fujiwara. 1994. T cell activation-associated hepatic injury: mediation by tumor necrosis factors and protection by interleukin 6. *J. Exp. Med. 179:1529.*
30. Carnaud, C., D. Lee, O. Donnars, S.-H. Park, A. Beavis, Y. Koezuka, and A. Bendelac. 1999. Cross-talk between cells of the innate immune system: NKT cells rapidly activate NK cells. *J. Immunol. 163:4647.*
31. Gantner, F., M. Leist, A. W. Lohse, P. G. Germann, and G. Tiegs. 1995. Concanavalin A-induced T-cell-mediated hepatic injury in mice: the role of tumor necrosis factor. *Hepatology 21:190.*
32. Chen, H., H. Huang, and W. E. Paul. 1997. NK1.1$^+$ CD4$^+$ T cells lose NK1.1 expression upon in vitro activation. *J. Immunol. 158:5112.*
33. Wilson, M. T., C. Johansson, D. Olivares-Villagómez, A. K. Singh, A. K. Stanic, C.-R. Wang, S. Joyce, M. J. Wick, and L. van Kaer. 2003. The response of natural killer T cells to glycolipid antigens is characterized by surface receptor down-modulation and expansion. *Proc. Natl. Acad. Sci. USA 100:10913.*
34. Crowe, N. Y., A. P. Uldrich, K. Kyparissoudis, K. J. L. Hammond, Y. Hayakawa, S. Sidobre, R. Keating, M. Kronenberg, M. J. Smyth, and D. I. Godfrey. 2003. Glycolipid antigen drives rapid expansion and sustained cytokine production by NK T cells. *J. Immunol. 171:4020.*
35. Emoto, M., and S. H. E. Kaufmann. 2003. Liver NKT cells: an account of heterogeneity. *Trends Immunol. 24:364.*
36. Kronenberg, M., and L. Gapin. 2002. The unconventional lifestyle of NKT cells. *Nat. Rev. Immunol. 2:557.*
37. Lafoux, V., L. Beaudoin, D. Jeske, C. Carnaud, and A. Lehuen. 2001. NK T cell-induced protection against diabetes in Vα14-Jα281 transgenic nonobese diabetic mice is associated with a Th2 shift circumscribed regionally to the islets and functionally to islet autoantigen. *J. Immunol. 166:3749.*
38. Gunperz, J. E., S. Miyake, T. Yamamura, and M. B. Brenner. 2002. Functionally distinct subsets of CD1d-restricted natural killer T cells revealed by CD1d tetramer staining. *J. Exp. Med. 195:625.*
39. Lee, P. T., K. Benlagha, L. Teyton, and A. Bendelac. 2002. Distinct functional lineages of human Vα24 natural killer T cells. *J. Exp. Med. 195:637.*
40. Chen, H., and W. E. Paul. 1997. Cultured NK1.1$^+$ CD4$^+$ T cells produce large amounts of IL-4 and IFN-γ upon activation by anti-CD3 or CD1. *J. Immunol. 159:2240.*
41. Pellicci, D. G., K. J. L. Hammond, A. P. Uldrich, A. G. Baxter, M. J. Smyth, and D. I. Godfrey. 2002. A natural killer T (NKT) cell developmental pathway involving a thymus-dependent NK1.1$^-$ CD4$^+$ CD1d-dependent precursor stage. *J. Exp. Med. 195:835.*
42. Benlagha, K., T. Kyin, A. Beavis, L. Teyton, and A. Bendelac. 2002. A thymic precursor to the NK T cell lineage. *Science 296:553.*

Critical roles of interferon regulatory factor 4 in CD11b^{high}CD8α^- dendritic cell development

Shoichi Suzuki*, Kiri Honma†, Toshifumi Matsuyama‡§, Kazuo Suzuki¶, Kan Toriyama‖, Ichinose Akitoyo**, Kazuo Yamamoto‡, Takashi Suematsu††, Michio Nakamura*, Katsuyuki Yui†, and Atsushi Kumatori*

Departments of *Host-Defense Biochemistry and ‖Pathology, **Central Laboratory, Institute of Tropical Medicine, †Division of Immunology, Department of Translational Medical Sciences, ‡Department of Molecular Microbiology and Immunology, and ††Electron Microscope Center, Graduate School of Biomedical Sciences, Nagasaki University, 1-12-4 Sakamoto, Nagasaki 852-8523, Japan; and ¶Laboratory of Biodefense, National Institute of Infectious Diseases, 1-23-1 Toyama, Shinjuku-ku, Tokyo 162-8640, Japan

Edited by Ralph M. Steinman, The Rockefeller University, New York, NY, and approved April 27, 2004 (received for review March 29, 2004)

IFN regulatory factors (IRFs) are a family of transcription factors that play an essential role in the homeostasis and function of immune systems. Recent studies indicated that IRF-8 is critical for the development of CD11b^{low}CD8α^+ conventional dendritic cells (DCs) and plasmacytoid DCs. Here we show that IRF-4 is important for CD11b^{high}CD8α^- conventional DCs. The development of CD11b^{high} DCs from bone marrow of IRF-4$^{-/-}$ mice was severely impaired in two culture systems supplemented with either GM-CSF or Flt3-ligand. In the IRF-4$^{-/-}$ spleen, the number of CD4$^+$CD8α^- DCs, a major subset of CD11b^{high} DCs, was severely reduced. IRF-4 and IRF-8 were expressed in the majority of CD11b^{high}CD4$^+$CD8α^- DCs and CD11b^{low}CD8α^+ DCs, respectively, in a mutually exclusive manner. These results imply that IRF-4 and IRF-8 selectively play critical roles in the development of the DC subsets that express them.

Dendritic cells (DCs) are professional antigen-presenting cells that link the innate and adaptive immune systems. They express CD11c and are composed of heterogeneous cell populations with different functions (1). At present, murine DCs have been divided into two major groups, B220$^-$ conventional DCs and B220$^+$ plasmacytoid DCs (2–5). In lymphoid organs, the conventional DCs can be divided into two subsets, CD11b^{high}CD8α^- and CD11b^{low}CD8α^+ DCs, based on the expression of surface markers (1). In the spleen, the CD11b^{high}CD8α^- subset can be further divided into CD4$^+$ and CD4$^-$ DCs (6, 7). *In vitro*, CD11b^{high}CD8α^- DCs can be generated in two bone marrow (BM) culture systems, supplemented with either granulocyte–macrophage colony-stimulating factor (GM-CSF) or Flt3 ligand (Flt3L) (8–10). CD11b^{low}CD8α^+ DCs can also be generated from a BM culture supplemented with Flt3L, although further stimulation by lipopolysaccharide (LPS) is needed to induce the expression of CD8α (10). The molecular phenomena that regulate the differentiation of these distinct subsets of DCs are poorly understood.

Transcription factors of the IFN-regulatory factor (IRF) family participate in the early host response to pathogens, immunomodulation, and hematopoietic differentiation (11). A member of the family, IRF-4, was cloned independently as a homologous member of the IRF gene family (12) and as an interacting partner of PU.1 (Pip) (13). PU.1 is an Ets family member involved in B lymphocyte and myeloid lineage development (14, 15) and is essential for the development of CD8α^- DCs (16, 17). Upon their association, IRF-4 and PU.1 undergo conformational changes, followed by binding to the DNA-binding element (18). IRF-4 is expressed at all stages of B cell development, in mature T cells (12), adult T cell leukemia cell lines (19, 20), and in macrophages (21, 22). The analysis of mice lacking IRF-4 (IRF-4$^{-/-}$) revealed that IRF-4 is essential for the function and homeostasis of both mature B and T lymphocytes (23, 24). IRF-8 (originally named IFN consensus sequence binding protein, ICSBP) is another member of the IRF family, and its structure is closely related to that of IRF-4. It can interact with PU.1 and binds to a DNA sequence similar to that bound by IRF-4 (22). Recent studies indicated that IRF-8 is critical for the development of CD11b^{low}CD8α^+ conventional DCs and plasmacytoid DCs (25–28). Here, we show that bone marrow cells from IRF-4 knockout mice have intrinsic defects in the development of CD11b^{high} DCs in two culture systems supplemented with either GM-CSF or Flt3-ligand. Mice lacking the IRF-4 gene have selective defects in splenic CD11b^{high}CD8α^- conventional DCs. IRF-4 is expressed in this subset of DCs, indicating that IRF-4 plays a critical role in the development of the DC subset that expresses it.

Methods

Mice. C57BL/6J mice were purchased from CLEA Japan (Osaka). IRF-4-deficient mice (23) and OT-II transgenic mice (29), expressing the T cell receptor specific for OVA323–339 and I-A^b, were maintained at the Laboratory Animal Center for Biomedical Research, Nagasaki University School of Medicine.

BM Cultures. The GM-CSF-supplemented BM culture was performed as described (9). The culture supernatant from a Chinese hamster ovary cell line transfected with the murine GM-CSF gene was used as the source of GM-CSF. At day 10, the nonadherent cells were harvested by gentle pipeting and were stimulated with 1 μg/ml LPS (*Escherichia coli* 0127:B8, Sigma) for 48 h. The Flt3L-supplemented BM culture was performed as described (10), except mouse Flt3L (Genzyme/Techne) was used. At day 9, the nonadherent cells were harvested by gentle pipeting and were stimulated with 1 μg/ml LPS for 24 h. For the experiments using the six-well transwell plates (Corning, NY), 5.2×10^5 BM cells (low cell density) in the lower chamber and 5×10^6 BM cells (high cell density) in the upper chamber were cultured in 4.1 ml of McCoy's medium, supplemented with 100 ng/ml Flt3L, for 10 days as described (10). For details see *Supporting Text*, which is published as supporting information on the PNAS web site.

Cell Preparation from Lymphoid Organs. Cells from thymuses and spleens were prepared as described (6). Low-density cells from spleen were also prepared as described (6).

Flow Cytometry. The cells were blocked with anti-CD16/32 antibody, rat IgG, and mouse IgG. All antibodies were purchased from BD Pharmingen, except where noted. In addition to the isotype controls, the following antibodies were used: Anti-CD16/32, FITC-conjugated anti-MHC class II (MHC-II),

This paper was submitted directly (Track II) to the PNAS office.

Abbreviations: DC, dendritic cell; BM, bone marrow; Flt3L, Flt3 ligand; GM-CSF, granulocyte–macrophage colony-stimulating factor; LPS, lipopolysaccharide; IRF, IFN-regulatory factor; PE, phycoerythrin; PerCP, peridinin chlorophyll-α protein; NPTII, neomycin phosphotransferase II; OVA, ovalbumin; MHC-II, MHC class II; NK, natural killer.

§To whom correspondence should be addressed. E-mail: tosim@net.nagasaki-u.ac.jp.

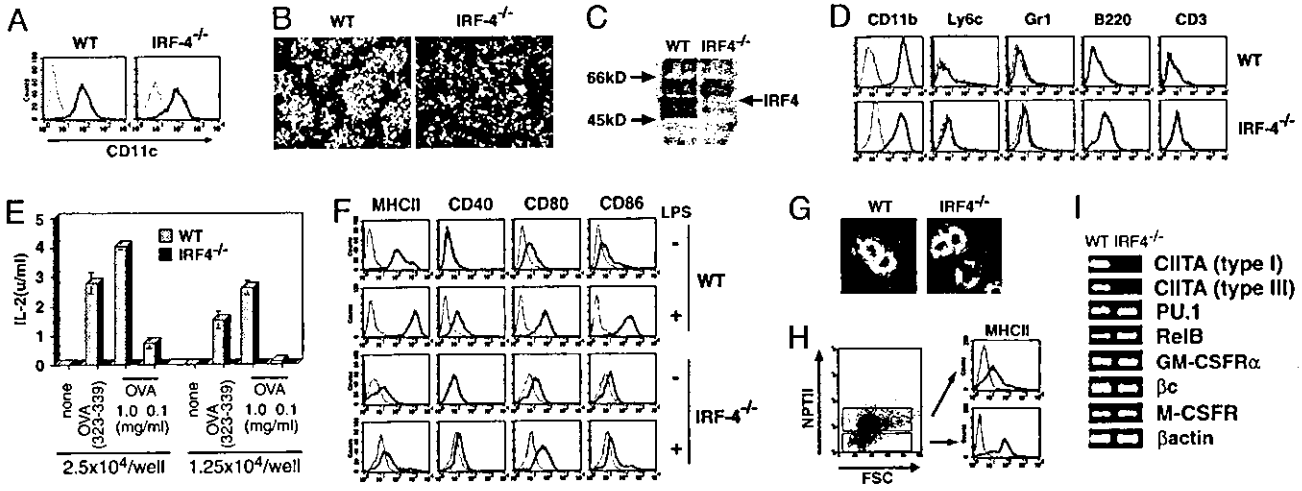

Fig. 1. Impaired DC development in the IRF-4$^{-/-}$ BM culture with GM-CSF. (*A*) The CD11c expression on nonadherent cells from GM-CSF BM cultures at day 10 was analyzed by flow cytometry. (*B*) Photographs of the cultures by phase contrast microscopy, taken at day 10. (*C*) The expression of IRF-4 in the CD11c$^+$ cells was assessed by immunoblotting. Lysates from 2.5 × 10^5 cells were subjected to electrophoresis. (*D*) The lineage marker expression on the CD11c$^+$ cells was analyzed by flow cytometry. (*E*) The antigen-presenting ability of the CD11c$^+$ cells for whole OVA and its peptide (323–339 amino acid residues) to OVA-specific CD4$^+$ T cells was examined. (*F*) MHC-II and costimulatory factor expression by the nonstimulated and LPS-stimulated CD11c$^+$ cells was examined. (*G*) The morphology of LPS-stimulated CD11c$^+$ cells was observed by phase contrast microscopy. (*H*) Wild-type and IRF-4$^{-/-}$ BM cells were cocultured. After 10 days, the expression of MHC-II on the cells was analyzed. NPTII expression by the wild-type and the IRF-4$^{-/-}$ cells was distinguished by flow cytometry with anti-MHC-II and anti-NPTII. (*I*) The expression of several transcription factor and cytokine receptor genes involved in DC development was analyzed by RT-PCR.

anti-CD8, and anti-Gr-1; phycoerythrin (PE)-conjugated anti-CD11c; CyChrome-conjugated anti-CD4; peridinin chlorophyll-α protein (PerCP)-conjugated anti-B220; biotin-conjugated anti-CD11b, anti-B220, and anti-Ly6c; PE-conjugated anti-CD40, anti-CD80, and anti-CD86 from Immunotech; biotin-conjugated anti-CD8 and anti-MHC-II, PE-conjugated anti-CD3, and allophycocyanin-conjugated anti-CD4 from eBioscience; and anti-IRF-4 and anti-IRF-8 from Santa Cruz Biotechnology. The binding of biotinylated antibodies was detected with PerCP-Cy5.5- or CyChrome-conjugated streptavidin. Analyses of stained cells were performed on a FACScan or FACSCalibur with the CELLQUEST software (BD Bioscience).

Intracellular Staining. For the analysis of neomycin phosphotransferase II (NPTII), cells were fixed and permeabilized with the Fix and Perm kit (Caltag), and were incubated with anti-NPTII (Upstate Biotechnology) followed by ant-rabbit IgG-biotin (Santa Cruz Biotechnology) and streptavidin-CyChrome. For analyses of IRF-4 and IRF-8, cells were fixed with 1% paraformaldehyde (Wako) and permeabilized with 0.5% Triton X-100 (Wako). The permeabilized cells were incubated with the anti-IRF-4 or IRF-8 antibody, followed by anti-goat IgG-Alexa Fluor 488 (Molecular Probes)

Western Blot Analysis. Cell lysates were prepared as described (30), with modifications (see supporting information). Immunoblotting was performed as described (31).

RT-PCR. Total RNA was prepared from cells as described (31). The cDNA synthesized from the total RNA by using ReverTra Ace (Toyobo) was subjected to PCR amplification using EX *Taq* (Takara) and the following primers: CIITA (sense), type I exon1: GACTTTCTTGAGCTGGGTCTG; type III exon1: CTGGCCCTTCTGGGTCTTAC; CIITA (antisense), common exon2: TCTTCATCCAGTTCCATGTCC. All of the other primer sequences are available on request.

Antigen-Presentation Assay. The ability of DCs to activate antigen-specific T cells was monitored by the secretion of IL-2 from CD4$^+$ T cells of OT-II mice. Purified CD4$^+$ T cells from OT-II mice (4 × 10^5 per well) were stimulated with ovalbumin (OVA) or its peptide and various numbers of DCs. After 48 h, the IL-2 level in the culture supernatant was determined by a sandwich ELISA with a biotin-conjugated anti-IL-2 antibody (BD Pharmingen) and avidin-alkaline phosphatase (Jackson ImmunoResearch).

Results

Defective DC Development in IRF-4$^{-/-}$ BM Culture. During analyses of the DC-specific regulatory mechanisms of the gp91^{phox} gene, which is expressed in a cell type-specific manner (32–34), we found that the IRF-4 protein was expressed in human DCs and bound to the Ets/IRF composite element of the promoter together with PU.1 (data not shown). This observation was consistent with the recent studies on DC-associated factors, which revealed the expression of IRF-4 mRNA in human DCs (35, 36). Therefore, we used the GM-CSF-supplemented cultures of BM from IRF-4$^{-/-}$ mice to determine the role of IRF-4 in DC development and function. Nonadherent CD11c$^+$ cells were generated from BM cells of IRF-4$^{-/-}$ mice as well as wild-type mice (Fig. 1*A*). Surprisingly, CD11c$^+$ cells from IRF-4$^{-/-}$ BM failed to form DC clusters (Fig. 1*B*) and showed no veil processes (Fig. 5, which is published as supporting information on the PNAS web site). A Western blot analysis demonstrated that CD11c$^+$ cells from wild-type mice expressed the IRF-4 protein, but those from IRF-4$^{-/-}$ mice did not (Fig. 1*C*). Flow cytometry analysis showed that CD11c$^+$ cells from both wild-type and IRF-4$^{-/-}$ BM expressed CD11b at high levels but did not express B220, CD3, Gr-1, and Ly6c (Fig. 1*D*).

Next, we evaluated their ability to present the OVA protein (1 and 0.1 mg/ml) or its peptide (323–339 amino acid residues) to OVA-specific CD4$^+$ T cells from OT-II mice (29). The wild-type DCs stimulated IL-2 production of the T cells in antigen dose- and DC number-dependent manners. However, CD11c$^+$ cells from IRF-4$^{-/-}$ BM were unable to stimulate IL-2 production by OVA-specific T cells (Fig. 1*E*). We also analyzed their expression of the surface antigens associated with antigen presentation (Fig. 1*F*). The expression of MHC-II on CD11c$^+$ cells from IRF-4$^{-/-}$ BM was extremely low, consistent with their defects in

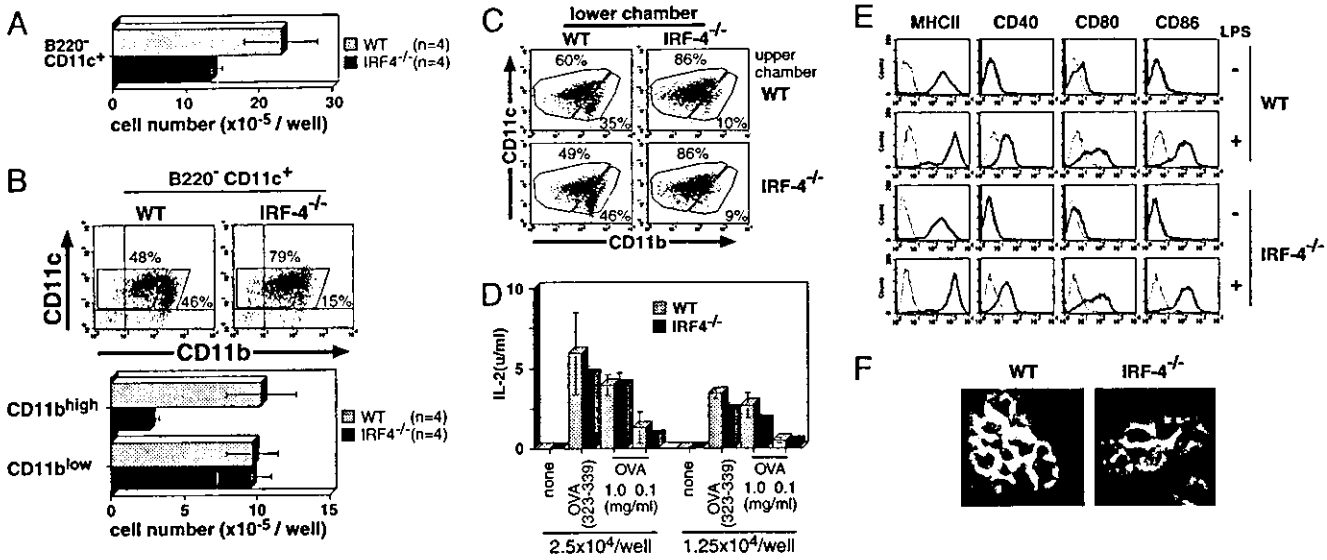

Fig. 2. Impaired development of the CD11b^{high} DC subset in the IRF-4$^{-/-}$ BM culture with Flt3L. Cells were stained with anti-CD11b-FITC, anti-CD11c-PE, and anti-B220-PerCP. (*A*) The number of B220$^-$CD11c$^+$ cells from IRF-4$^{-/-}$ BM was compared with that from wild-type BM cells at 9 days after culture. (*B*) Analysis of the DC subsets in the Flt3L culture was performed, based on the expression of B220, CD11b, and CD11c. The values (%) indicate the proportion of each DC subset to B220$^-$ cells (*Upper*). The number per well of CD11b^{low} and CD11b^{high} CD11c$^+$ DCs from IRF-4$^{-/-}$ BM cells was compared with that from wild-type BM cells (*Lower*). (*C*) Soluble factors from BM cells stimulated by Flt3L were assessed by using transwell plates. BM cells at low density (5.2×10^5 cells) were cultured in the lower chambers of transwell plates, separated by a 0.4-μm filter from BM cells at high density (5×10^6 cells) in the upper chambers. Analysis of the DC subsets in the lower chambers was performed, based on the expression of CD11b and CD11c. (*D*) The antigen-presenting ability was examined as described in Fig. 1*E*. (*E*) The expression of MHC-II and costimulatory factors on DCs was analyzed by flow cytometry. (*F*) The morphology of LPS-stimulated DCs was observed by phase-contrast microscopy.

antigen presentation. The expression of CD40, CD80, and CD86 on CD11c$^+$ cells from IRF-4$^{-/-}$ BM was similar to that of wild-type DCs. Strong up-regulation of the surface antigens was observed in wild-type DCs after stimulation with LPS. However, the up-regulation was not observed in most, if not all, CD11c$^+$ cells from IRF-4$^{-/-}$ BM. Morphologically, the CD11c$^+$ cells from IRF-4$^{-/-}$ BM did not develop the sheet-like veil structure after LPS stimulation (Fig. 1*G*). These results indicate that CD11c$^+$ cells from IRF-4$^{-/-}$ BM fail to respond normally to LPS.

To determine whether the impaired DC development of CD11c$^+$ cells from IRF-4$^{-/-}$ BM was caused by their intrinsic defects or environmental defects in the support of DC development in a GM-CSF-supplemented culture, we examined the generation of DCs from IRF-4$^{-/-}$ BM after a coculture with wild-type BM cells (Fig. 1*H*). The wild-type and IRF-4$^{-/-}$ BM could be distinguished by their expression of NPTII, whose gene was inserted when the IRF-4 gene was disrupted (23). Cells derived from IRF-4$^{-/-}$ BM cells (NPTII$^+$) in the mixed culture system did not express MHC-II at high levels, unlike those derived from wild-type BM (NPTII$^-$). This result indicates that the impaired DC development from IRF-4$^{-/-}$ BM cells is caused by cell autonomous defects.

To investigate the mechanisms underlying the impaired development of DCs from IRF-4$^{-/-}$ BM, we analyzed the mRNA expression of class II transactivator isoforms (CIITA types I and III), which are essential for the constitutive expression of MHC-II in DCs (37, 38) by an RT-PCR analysis. CD11c$^+$ cells from IRF-4$^{-/-}$ BM expressed the CIITA type I and III mRNAs at almost negligible levels, as compared with the wild-type DCs (Fig. 1*I*), which might be responsible for the low-MHC-II expression level. CD11c$^+$ cells from IRF-4$^{-/-}$ and wild-type BM expressed similar levels of the mRNAs encoding PU.1 and RelB, which are critical transcription factors for DC development (16, 17, 39, 40), the GM-CSF receptor components (α and cβ), and the M-CSF receptor, responsible for the interference of DC differentiation by M-CSF (41). Therefore, it is unlikely that the impaired DC development from IRF-4$^{-/-}$ BM cells is caused by the abnormal behaviors of PU.1 and RelB or abnormal responses to GM-CSF and M-CSF.

Defective Development Is Limited to CD11b^{high} DCs. We next used the Flt3L-supplemented BM culture system, which can give rise to B220$^+$CD11c$^+$ conventional DCs and B220$^+$CD11c$^+$ plasmacytoid DCs (42, 43). It is demonstrated that the conventional DCs from the culture contain two types of subsets, CD11b^{high} and CD11b^{low} DCs (10), and the plasmacytoid DCs do not express CD11b (42, 43). The number of B220$^-$CD11c$^+$ conventional DCs developed from IRF-4$^{-/-}$ BM was reduced to $\approx$60% of that produced by wild-type BM (Fig. 2*A*). The number of B220$^+$CD11c$^+$CD11b$^-$ plasmacytoid DCs that developed from IRF-4$^{-/-}$ BM, however, was similar to that from wild-type BM (Fig. 6, which is published as supporting information on the PNAS web site). We analyzed the expression of CD11b on B220$^-$CD11c$^+$ cells from the Flt3L-supplemented BM culture. The proportion of CD11b^{high} cells to CD11c$^+$ cells from the wild-type BM culture was 46%, whereas that from the IRF-4$^{-/-}$ BM was 15%. The absolute number of CD11c$^+$CD11b^{high} cells derived from IRF-4$^{-/-}$ BM was severely reduced, as compared with that from wild-type BM, whereas the absolute number of CD11c$^+$CD11b^{low} cells was unchanged (Fig. 2*B*). These results suggest that IRF-4 plays an important role in the development of CD11b^{high} conventional DCs, and is not essential for that of CD11b^{low} conventional DCs and plasmacytoid DCs in the Flt3L-supplemented BM culture. This defect of IRF-4$^{-/-}$ CD11b^{high} DCs could be due to the lack of soluble factor production by the IRF-4$^{-/-}$ BM cells. Therefore, we cultured IRF-4$^{-/-}$ and wild-type BM cells in the presence of Flt3L by using a transwell system as described (10). BM cells were cultured at low density in the lower chamber and at high density in the upper chamber in the presence of Flt3L (Fig. 2*C*). At the end of the culture, the generation of DCs in the lower chamber was analyzed by flow

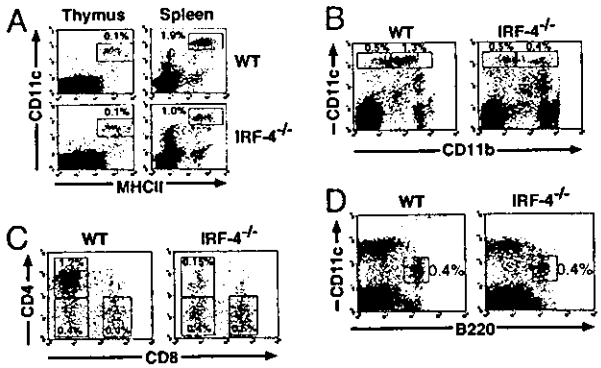

Fig. 3. Splenic CD11b^{high}CD4^{+}CD8α^{-} conventional DCs are selectively reduced in IRF-4$^{-/-}$ mice. Six-week-old male mice were used. (*A*) Thymic and splenic cells were stained with anti-MHC-II-FITC, anti-CD11c-PE, and anti-B220-PerCP. The CD11c^{high}MHC-II^{high} cells were analyzed after the B220^{+} population was electrically gated out. (*B*) Splenic cells were stained with anti-CD11b-FITC, anti-CD11c-PE, and anti-B220-PerCP. Expression of CD11b on CD11c^{high} DCs was analyzed after the B220^{+} population was electrically gated out. (*C*) Splenic cells were stained with anti-CD8α FITC, anti-CD11c-PE, and anti-CD4-CyChrome, and then the expression of CD4 and CD8α on CD11c^{high} DCs was analyzed. (*D*) Splenic cells were stained with anti-CD19-FITC and anti-NK1.1-FITC, anti-CD11c-PE, and anti-B220-biotin. The CD11c versus B220 profile is shown, after the CD19- or NK1.1-positive populations were electrically gated out to exclude B and NK cells. The biotinylated B220 antibody was detected with streptavidin-PerCP-Cy5.5. The values (%) indicate the proportion of gated populations to total thymic or splenic cells.

cytometry. In this system, the development of DCs from the wild-type BM cells in the lower chamber depended on the presence of wild-type BM cells at high density in the upper chamber (S.S. and A.K., unpublished data). Wild-type BM cells gave rise to a CD11c^{+}CD11b^{high} population when IRF-4$^{-/-}$ BM cells were cultured in the upper chamber (Fig. 2*C Lower Left*), suggesting that IRF-4$^{-/-}$ BM cells generated soluble factors that support DC development from the wild-type BM in the presence of Flt3L. On the contrary, the proportion of the CD11b^{high} population derived from IRF-4$^{-/-}$ BM cells remained low, even after they were cultured with wild-type BM in the upper chamber at high density (Fig. 2*C Upper Right*). Taken together, these results suggest that the defect in the generation of a CD11c^{+}CD11b^{high} population from IRF-4$^{-/-}$ BM in the presence of Flt3L is an intrinsic characteristic of these cells.

Next, we examined the properties of the CD11c^{+} cells generated from IRF-4$^{-/-}$ BM in the Flt3L-supplemented culture. The CD11c^{+} cells from IRF-4$^{-/-}$ BM were able to present whole OVA and its peptide (323–339 amino acid residues) to naive CD4^{+} T cells from OT-II mice (Fig. 2*D*). They expressed MHC-II, CD40, CD80, and CD86 on the cell surface at levels similar to those of DCs from wild-type BM, before and after LPS stimulation (Fig. 2*E*). The CD11c^{+} cells from IRF-4$^{-/-}$ and wild-type BM were morphologically indistinguishable (Fig. 2*F*). Because the majority of the IRF-4$^{-/-}$ DCs were CD11b^{low} conventional DCs (Figs. 2*B* and 6), these results suggest that the CD11b^{low} DCs in IRF-4$^{-/-}$ DCs are not impaired in their antigen-presenting function and responsiveness to LPS.

Defects of CD11b^{high} DCs in IRF-4$^{-/-}$ Spleen. Next, we examined the levels of conventional DCs *in vivo*. The majority of thymic and splenic conventional DCs belong to the CD11b^{low} and CD11b^{high} DC subsets, respectively (1). The proportion of conventional DCs in the thymus of IRF-4$^{-/-}$ mice was similar to that of the wild-type (0.1%), whereas it was reduced by ≈50% in the spleen (Fig. 3*A*). Among these DCs in the spleen, the proportion of CD11b^{high} DCs was markedly reduced, whereas that of CD11b^{low} DCs was not (Fig. 3*B*). Because the total splenic cell numbers

Table 1. Reduced number of CD4^{+}CD8^{-} DCs in IRF-4$^{-/-}$ spleen

	Wild type	IRF-4$^{-/-}$
Splenocytes	1,040 ± 240	1,030 ± 190
CD11c^{high}MHC-II^{+}	22.5 ± 3.2	11.7 ± 3.1
CD11b^{high}CD4^{+}CD8^{-}	12.8 ± 2.1	1.5 ± 0.5
CD11b^{high}CD4^{-}CD8^{-}	4.6 ± 1.2	5.0 ± 1.3
CD11b^{low}CD4^{-}CD8^{+}	4.9 ± 1.0	5.1 ± 1.5
CD11c^{int}B220^{+}	5.1 ± 1.5	4.4 ± 0.5

Results represent the number of cells per spleen. Values are the means ± SD (×10^{-5}) of eight mice aged 6 weeks.

were comparable (Table 1), the absolute number of CD11b^{high} DCs was selectively reduced in the IRF-4$^{-/-}$ spleen, consistent with the essential role of IRF-4 in the generation of CD11b^{high} DCs *in vitro*. Splenic CD11b^{high} DCs can be further subdivided into CD4^{+}CD8α^{-} and CD4^{-}CD8α^{-} subsets (6, 7). We further classified the splenic DCs, based on the expression of CD4 and CD8α. Flow cytometry analyses revealed that the CD4^{+}CD8α^{-} splenic DCs in IRF-4$^{-/-}$ mice were selectively reduced to ≈10% of the number in wild-type mice (Fig. 3*C*). As shown in Table 1, the absolute number of CD4^{+}CD8α^{-} DCs in the IRF-4$^{-/-}$ spleen was ≈10% of that found in the wild-type, resulting in the lower total number of CD11c^{high}MHC-II^{+} DCs. These results demonstrated that the splenic CD11b^{high}CD4^{+}CD8α^{-} subset was selectively reduced among the conventional DCs in the IRF-4$^{-/-}$ mouse. We also examined the level of plasmacytoid DCs in the IRF-4$^{-/-}$ spleen. CD19^{+}and NK1.1^{+} cells were gated out to exclude B cells and natural killer (NK) cells, which are B220^{+} and CD11c^{low}, respectively (44). The proportion and the absolute number of CD11c^{int}B220^{+} plasmacytoid DCs in IRF-4$^{-/-}$ spleen were not significantly different from those of the wild-type spleen (Fig. 3*D* and Table 1). Taken together, these results suggest that IRF-4 is critical for the development of the majority of CD11b^{high}CD4^{+}CD8α^{-} splenic conventional DCs, but not for that of CD11b^{high}CD4^{-}CD8α^{-} and CD11b^{low}CD4^{-}CD8α^{+} splenic conventional DCs as well as plasmacytoid DCs.

IRF-4/IRF-8 Expression in Distinct DC Subsets. We next analyzed the expression of IRF-4 and IRF-8 in each splenic conventional DC subset at the single cell level, using four-color flow cytometry after triple staining of cell surface markers and intracellular IRFs (Fig. 4*A*). IRF-8 is another member of the IRF family that is important for DC development (25–28). In the wild-type spleen, all of the CD4^{+}CD8α^{-} DCs expressed IRF-4 and a small population (≈15%) expressed IRF-8, indicating that most of the CD4^{+}CD8α^{-} DCs express IRF-4 alone, and a minor population expresses both IRFs. In contrast, the majority of CD4^{-}CD8α^{+} DCs in the wild-type spleen expressed IRF-8 and only ≈10% expressed IRF-4, indicating that most CD4^{-}CD8α^{+} DCs express IRF-8, but not IRF-4. The majority of CD4^{-}CD8α^{-} splenic DCs expressed IRF-4 in wild-type mice, whereas ≈40% expressed IRF-8. In the IRF4$^{-/-}$ mouse spleen, all of the CD4^{-}CD8α^{+} DCs expressed IRF-8, as expected. Interestingly, the small population of CD4^{+}CD8α^{-} DCs that remained in IRF4$^{-/-}$ mice expressed IRF-8, unlike the majority of these cells in wild-type mice. In addition, the majority of the CD4^{-}CD8α^{-} DCs, of which ≈60% did not express IRF-8 in wild-type mice, also expressed IRF-8 in the IRF-4$^{-/-}$ spleen. Taken together, these results indicate that the IRF-4 defect specifically affected the CD4^{+}CD8α^{-} and CD4^{-}CD8α^{-} DC subsets, which both preferentially expressed IRF-4 in wild-type mice.

The expression levels of IRF-4 and -8 in CD11c^{+} cells from the BM culture with GM-CSF were analyzed by flow cytom-

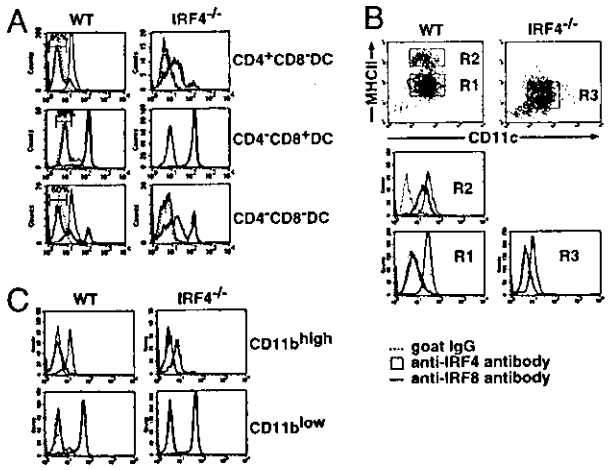

Fig. 4. IRF-4 and IRF-8 expression in various DC subsets. (*A*) Flow cytometric analysis of IRF-4 and IRF-8 expression in splenic conventional DCs. After low-density cells from wild-type and IRF-4$^{-/-}$ spleen were stained with anti-CD11c-PE, anti-CD4-allophycocyanin, and anti-CD8α-PerCP-Cy5.5, the cells were fixed, permeabilized, and stained with anti-IRF-4 or anti-IRF-8, followed by the Alexa Fluor 488-conjugated second antibody. CD11c^{high} DCs were gated on, and divided into the three subsets. Each subset was gated on, and IRF-4 and IRF-8 expression was examined. (*B*) Flow cytometric analysis of IRF-4 and IRF-8 expression in DCs from the GM-CSF culture. The wild-type and IRF-4$^{-/-}$ DCs were stained with anti-MHC-II-biotin and anti-CD11c-PE, followed by intracellular staining as described in *A*. (*C*) Flow cytometric analysis of IRF-4 and IRF-8 expression in DCs from the Flt3L culture. The wild-type and IRF-4$^{-/-}$ DCs were stained with anti-CD11b-biotin and anti-CD11c-PE, followed by intracellular staining as described in *A*. Cells were divided into CD11b^{high} and CD11b^{low} DCs as shown in Fig. 2*A*. Each population was gated on, and IRF-4 and IRF-8 expression was examined. The biotinylated antibodies used in *B* and *C* were detected with streptavidin-PerCP-Cy5.5.

etry (Fig. 4*B*). IRF-4 was expressed in both immature (R1) and mature (R2) wild-type DCs. However, IRF-8 was not expressed in immature wild-type DCs, suggesting a role of IRF-8 in the maturation of wild-type DCs, as reported (25–27), but not for their development in the GM-CSF-supplemented culture. The stimulation of the immature DCs with LPS induced IRF-8 expression, concomitant with their maturation (data not shown). In contrast, the majority of CD11c^{+} cells from IRF-4$^{-/-}$ BM (R3) expressed IRF-8. The aberrant expression of IRF-8 in these cells was insufficient to compensate for the lack of IRF-4, because these cells were unable to become functional DCs (Fig. 1).

We also analyzed the expression of IRF-4 and -8 in CD11b^{high} and CD11b^{low} DCs from the BM culture with Flt3L (Fig. 4*C*). The majority of CD11b^{high} cells from wild-type BM expressed IRF-4, but not IRF-8, whereas the majority CD11b^{low} cells expressed IRF-8, but not IRF-4. Interestingly, the majority of CD11b^{high} cells that were generated from IRF-4$^{-/-}$ BM expressed significant levels of IFR-8, unlike those derived from wild-type BM. This result is consistent to the *in vivo* observation that most CD11b^{high} splenic DCs express IRF-8 in the IRF-4$^{-/-}$ mouse (Fig. 4*A*).

Discussion

In the present study, we demonstrated that IRF-4 is important for most DCs of the CD11b^{high}CD8α^{-} subset, but not of the CD11b^{low}CD8α^{+} subset. We show that IRF-4 is expressed in most DCs of the CD11b^{high}CD8α^{-} subset, but not of CD11b^{low}CD8α^{+} subset in mouse spleen. The expression of IRF-4 in this DC subset was also confirmed in two BM culture systems. The DCs derived from BM in the presence of GM-CSF were uniformly CD11b^{high}, and most of them expressed IRF-4. Both CD11b^{high} and CD11b^{low} conventional DCs developed from BM in cultures supplemented with Flt3L; however, IRF-4 was preferentially expressed in the CD11b^{high} DC populations. Studies with mice lacking IRF-4 also determined that IRF-4 plays a critical role in these DC subsets. The development of CD11b^{high} DCs from IRF-4$^{-/-}$ BM *in vitro* was severely impaired in both culture systems. Furthermore, the number of CD4^{+}CD8α^{-} DCs, a major subset of CD11b^{high} DCs, was severely reduced in the spleen in mice lacking IRF-4. These results indicate that IRF-4 is selectively expressed in the CD11b^{high} subset of conventional DCs and plays critical roles in their development.

Comparative analyses of the expression of IRF-4 and IRF-8 in DCs revealed that conventional DCs can be grouped into three subpopulations: IRF-4(+)IRF-8(−), IRF-4(−)IRF-8(+), and IRF-4(+)IRF-8(+). The IRF-4(+)IRF-8(−) subpopulation preferentially belongs to the both CD11b^{high}CD4^{+} and CD11b^{high}CD4^{-} subsets, whereas the IRF-4(−)IRF-8(+) subpopulation preferentially belongs to the CD11b^{low}CD8^{-} DC subset. This observation may yield insight into the complicated developmental pathways of DCs. In mice lacking IRF-4, most of the DCs in CD11b^{high}CD8^{-} subset expressed IRF-8, although the majority of the DCs in this subset did not express IRF-8 in the wild-type mouse. These results suggest that a subset of IRF-8(−) DCs could not be generated in the absence of the IRF-4 gene, implying that IRF-4 is essential for the development of IRF-8(−), but not IRF-8(+), DCs. In contrast to the CD11b^{high} DC subsets, we did not detect any significant abnormality in the CD11b^{low}CD8α^{+} DCs in IRF-4$^{-/-}$ mice. This subpopulation of DCs in the spleens of wild-type and IRF-4$^{-/-}$ mice is IRF-8(+). The DCs that develop from the BM of IRF-4$^{-/-}$ mice in the Flt3L-supplemented culture are also IRF-8(+), suggesting that IRF-4 is not essential for the development and maturation of CD11b^{low}CD8α^{+} conventional DCs. Taken together, it is clear that all of the DC subsets that were examined expressed IRF-4 and/or IRF-8, suggesting the intriguing possibility that the function of either IRF-4 or IRF-8 is essential for the development of DCs.

The development of CD11b^{high} CD4^{+} DCs was severely impaired in mice lacking the RelB subunit of NF-κB (45). This defect in the DC subset is similar to the defects in IRF-4$^{-/-}$ mice. The expression of the IRF-4 gene is activated by c-Rel, another member of the NF-κB family, in B cells (46). RelB can bind to the same recognition DNA sequence as c-Rel in DCs (47). These findings suggest that IRF-4 might be regulated by RelB in DCs. In addition, tumor necrosis factor receptor-associated factor (TRAF) 6, which operates in the activation of NF-κB, is required for the development of conventional CD4^{+} DCs (45), suggesting that IRF-4 might also be regulated through TRAF6. The elucidation of the regulatory mechanisms for IRF-4 gene expression would help to clarify the developmental mechanisms of DCs.

Functional differences between CD11b^{high}CD8α^{-} and CD11b^{low}CD8α^{+} DCs have been suggested in a number of studies. These two subclasses of DCs regulate the development of T helper (Th) cells secreting discrete sets of lymphokines: CD11b^{high}CD8α^{-} DCs induce Th2-type responses and CD11b^{low}CD8α^{+} DCs induce Th1-type responses (48). The preferential induction of Th1 responses by CD11b^{low}CD8α^{+} DCs is mainly caused by their production of IL-12. In this study, we showed that IRF-4 and IRF-8 are expressed preferentially in CD11b^{high}CD8α^{-} and CD11b^{low}CD8α+ DCs, respectively. These IRFs may dictate not only the differentiation but also the function of these DC subsets. IRF-8 directs the expression of IL-12 (49) and IL-18 (50), promoting Th1-biased immune responses. On the other hand, IRF-4 is involved in the Th2-bias, by promoting IL-4 production by CD4^{+} T-cells and regulating their responsiveness to IL-4 (24, 51, 52). Therefore, it is intriguing to speculate that the IRF-4 expressed

in the CD11b^{high}CD8α^- subset of DCs is involved in Th2-biased immune responses, by inducing certain Th2-promoting cytokines. In addition, the IRF-4 expressed in B cells is critical for their Ab production, further supporting the role of IRF-4 in humoral immune responses (23). Taken together, these results strongly suggest that the IRF-4 expressed in T and B lymphocytes, as well as in the CD11b^{high}CD8α^- subset of DCs, is a crucial transcription factor for promoting humoral immune responses. In other words, IRF-4 polarizes the Th2 response extrinsically as well as intrinsically. Further analyses of DCs and DC precursors, based on the expression and functions of IRF members, should provide important insights into the present controversy regarding both the developmental origin of DCs and the functional distinctions among DC subsets.

We thank T. Moriuch and M. Nakamura for animal care and Drs. W. Heath and H. Kosaka for providing the OT-II mice. We also thank Dr. T. Sudo for the GM-CSF-producing and -indicator cells, Drs. K. Yamashita and K. Miyazaki for technical advice, and Dr. S. Yoshinaga for helpful discussions and comments. This work was supported by 21st Century COE Program of Nagasaki University and a Grant-in-Aid for Young Scientist (B) from the Ministry of Education, Culture, Sports, Science and Technology.

1. Shortman, K. & Liu, Y. J. (2002) *Nat. Rev. Immunol.* **2,** 151–161.
2. Bjorck, P. (2001) *Blood* **98,** 3520–3526.
3. Asselin-Paturel, C., Boonstra, A., Dalod, M., Durand, I., Yessaad, N., Dezutter-Dambuyant, C., Vicari, A., O'Garra, A., Biron, C., Briere, F. & Trinchieri, G. (2001) *Nat. Immunol.* **2,** 1144–1150.
4. Nakano, H., Yanagita, M. & Gunn, M. D. (2001) *J. Exp. Med.* **194,** 1171–1178.
5. Ardavin, C. (2003) *Nat. Rev. Immunol.* **3,** 582–590.
6. Vremec, D., Pooley, J., Hochrein, H., Wu, L. & Shortman, K. (2000) *J. Immunol.* **164,** 2978–2986.
7. Martin, P., del Hoyo, G. M., Anjuere, F., Ruiz, S. R., Arias, C. F., Marin, A. R. & Ardavin, C. (2000) *Blood* **96,** 2511–2519.
8. Inaba, K., Inaba, M., Romani, N., Aya, H., Deguchi, M., Ikehara, S., Muramatsu, S. & Steinman, R. M. (1992) *J. Exp. Med.* **176,** 1693–1702.
9. Lutz, M. B., Kukutsch, N., Ogilvie, A. L., Rossner, S., Koch, F., Romani, N. & Schuler, G. (1999) *J. Immunol. Methods* **223,** 77–92.
10. Brasel, K., De Smedt, T., Smith, J. L. & Maliszewski, C. R. (2000) *Blood* **96,** 3029–3039.
11. Taniguchi, T., Ogasawara, K., Takaoka, A. & Tanaka, N. (2001) *Annu. Rev. Immunol.* **19,** 623–655.
12. Matsuyama, T., Grossman, A., Mittrucker, H. W., Siderovski, D. P., Kiefer, F., Kawakami, T., Richardson, C. D., Taniguchi, T., Yoshinaga, S. K. & Mak, T. W. (1995) *Nucleic Acids Res.* **23,** 2127–2136.
13. Eisenbeis, C. F., Singh, H. & Storb, U. (1995) *Genes Dev.* **9,** 1377–1387.
14. Scott, E. W., Simon, M. C., Anastasi, J. & Singh, H. (1994) *Science* **265,** 1573–1577.
15. McKercher, S. R., Torbett, B. E., Anderson, K. L., Henkel, G. W., Vestal, D. J., Baribault, H., Klemsz, M., Feeney, A. J., Wu, G. E., Paige, C. J. & Maki, R. A. (1996) *EMBO J.* **15,** 5647–5658.
16. Anderson, K. L., Perkin, H., Surh, C. D., Venturini, S., Maki, R. A. & Torbett, B. E. (2000) *J. Immunol.* **164,** 1855–1861.
17. Guerriero, A., Langmuir, P. B., Spain, L. M. & Scott, E. W. (2000) *Blood* **95,** 879–885.
18. Perkel, J. M. & Atchison, M. L. (1998) *J. Immunol.* **160,** 241–252.
19. Yamagata, T., Nishida, J., Tanaka, S., Sakai, R., Mitani, K., Yoshida, M., Taniguchi, T., Yazaki, Y. & Hirai, H. (1996) *Mol. Cell. Biol.* **16,** 1283–1294.
20. Imaizumi, Y., Kohno, T., Yamada, Y., Ikeda, S., Tanaka, Y., Tomonaga, M. & Matsuyama, T. (2001) *Jpn. J. Cancer Res.* **92,** 1284–1292.
21. Rosenbauer, F., Waring, J. F., Foerster, J., Wietstruk, M., Philipp, D. & Horak, I. (1999) *Blood* **94,** 4274–4281.
22. Marecki, S., Atchison, M. L. & Fenton, M. J. (1999) *J. Immunol.* **163,** 2713–2722.
23. Mittrucker, H. W., Matsuyama, T., Grossman, A., Kundig, T. M., Potter, J., Shahinian, A., Wakeham, A., Patterson, B., Ohashi, P. S. & Mak, T. W. (1997) *Science* **275,** 540–543.
24. Tominaga, N., Ohkusu-Tsukada, K., Udono, H., Abe, R., Matsuyama, T. & Yui, K. (2003) *Int. Immunol.* **15,** 1–10.
25. Schiavoni, G., Mattei, F., Sestili, P., Borghi, P., Venditti, M., Morse, H. C., III, Belardelli, F. & Gabriele, L. (2002) *J. Exp. Med.* **196,** 1415–1425.
26. Aliberti, J., Schulz, O., Pennington, D. J., Tsujimura, H., Reis e Sousa, C., Ozato, K. & Sher, A. (2003) *Blood* **101,** 305–310.
27. Tsujimura, H., Tamura, T., Gongora, C., Aliberti, J., Reis e Sousa, C., Sher, A. & Ozato, K. (2003) *Blood* **101,** 961–969.
28. Tsujimura, H., Tamura, T. & Ozato, K. (2003) *J. Immunol.* **170,** 1131–1135.
29. Barnden, M. J., Allison, J., Heath, W. R. & Carbone, F. R. (1998) *Immunol. Cell Biol.* **76,** 34–40.
30. Yu, D., Imajoh-Ohmi, S., Akagawa, K. & Kanegasaki, S. (1996) *J. Biochem. (Tokyo)* **119,** 23–28.
31. Kumatori, A., Yang, D., Suzuki, S. & Nakamura, M. (2002) *J. Biol. Chem.* **277,** 9103–9111.
32. Skalnik, D. G., Dorfman, D. M., Perkins, A. S., Jenkins, N. A., Copeland, N. G. & Orkin, S. H. (1991) *Proc. Natl. Acad. Sci. USA* **88,** 8505–8509.
33. Suzuki, S., Kumatori, A., Haagen, I. A., Fujii, Y., Sadat, M. A., Jun, H. L., Tsuji, Y., Roos, D. & Nakamura, M. (1998) *Proc. Natl. Acad. Sci. USA* **95,** 6085–6090.
34. Yang, D., Suzuki, S., Hao, L. J., Fujii, Y., Yamauchi, A., Yamamoto, M., Nakamura, M. & Kumatori, A. (2000) *J. Biol. Chem.* **275,** 9425–9432.
35. Hashimoto, S. I., Suzuki, T., Nagai, S., Yamashita, T., Toyoda, N. & Matsushima, K. (2000) *Blood* **96,** 2206–2214.
36. Ahn, J. H., Lee, Y., Jeon, C., Lee, S. J., Lee, B. H., Choi, K. D. & Bae, Y. S. (2002) *Blood* **100,** 1742–1754.
37. Chang, C. H., Guerder, S., Hong, S. C., van Ewijk, W. & Flavell, R. A. (1996) *Immunity* **4,** 167–178.
38. Muhlethaler-Mottet, A., Otten, L. A., Steimle, V. & Mach, B. (1997) *EMBO J.* **16,** 2851–2860.
39. Burkly, L., Hession, C., Ogata, L., Reilly, C., Marconi, L. A., Olson, D., Tizard, R., Cate, R. & Lo, D. (1995) *Nature* **373,** 531–536.
40. Wu, L., D'Amico, A., Winkel, K. D., Suter, M., Lo, D. & Shortman, K. (1998) *Immunity* **9,** 839–847.
41. Miyamoto, T., Ohneda, O., Arai, F., Iwamoto, K., Okada, S., Takagi, K., Anderson, D. M. & Suda, T. (2001) *Blood* **98,** 2544–2554.
42. Brawand, P., Fitzpatrick, D. R., Greenfield, B. W., Brasel, K., Maliszewski, C. R. & De Smedt, T. (2002) *J. Immunol.* **169,** 6711–6719.
43. Gilliet, M., Boonstra, A., Paturel, C., Antonenko, S., Xu, X. L., Trinchieri, G., O'Garra, A. & Liu, Y. J. (2002) *J. Exp. Med.* **195,** 953–958.
44. Lian, Z. X., Okada, T., He, X. S., Kita, H., Liu, Y. J., Ansari, A. A., Kikuchi, K., Ikehara, S. & Gershwin, M. E. (2003) *J. Immunol.* **170,** 2323–2330.
45. Kobayashi, T., Walsh, P. T., Walsh, M. C., Speirs, K. M., Chiffoleau, E., King, C. G., Hancock, W. W., Caamano, J. H., Hunter, C. A., Scott, P., *et al.* (2003) *Immunity* **19,** 353–363.
46. Grumont, R. J. & Gerondakis, S. (2000) *J. Exp. Med.* **191,** 1281–1292.
47. Boffa, D. J., Feng, B., Sharma, V., Dematteo, R., Miller, G., Suthanthiran, M., Nunez, R. & Liou, H. C. (2003) *Cell Immunol.* **222,** 105–115.
48. Maldonado-Lopez, R. & Moser, M. (2001) *Semin. Immunol.* **13,** 275–282.
49. Giese, N. A., Gabriele, L., Doherty, T. M., Klinman, D. M., Tadesse-Heath, L., Contursi, C., Epstein, S. L. & Morse, H. C., III (1997) *J. Exp. Med.* **186,** 1535–1546.
50. Kim, Y. M., Kang, H. S., Paik, S. G., Pyun, K. H., Anderson, K. L., Torbett, B. E. & Choi, I. (1999) *J. Immunol.* **163,** 2000–2007.
51. Rengarajan, J., Mowen, K. A., McBride, K. D., Smith, E. D., Singh, H. & Glimcher, L. H. (2002) *J. Exp. Med.* **195,** 1003–1012.
52. Lohoff, M., Mittrucker, H. W., Prechtl, S., Bischof, S., Sommer, F., Kock, S., Ferrick, D. A., Duncan, G. S., Gessner, A. & Mak, T. W. (2002) *Proc. Natl. Acad. Sci. USA* **99,** 11808–11812.

Nephrol Dial Transplant (2004) 19: 1708–1715
DOI: 10.1093/ndt/gfh275
Advance Access publication 18 May 2004

Nephrology
Dialysis
Transplantation

Original Article

Neutrophil contribution to the crescentic glomerulonephritis in SCG/Kj mice

Akiko Ishida-Okawara[1], Toshiko Ito-Ihara[1,2], Eri Muso[3], Takahiko Ono[2], Kan Saiga[4], Kyuichi Nemoto[4] and Kazuo Suzuki[1]

[1]Biodefense Laboratory, National Institute of Infectious Diseases, Toyama 1-23-1, Shinjuku-ku, Tokyo 162-8640, Japan, [2]Nephrology Division, Department of Cardiovascular Medicine, Graduate School of Medicine, Kyoto University, Kawara-cho 54, Shogoin, Sakyou-ku, Kyoto 606-8507, Japan, [3]Division of Nephrology and Dialysis, Kitano Hospital, The Tazuke Kofukai Medical Research Institute, 2-4-20 Ohgimachi, Kita-ku, Osaka 530-8480, Japan and [4]Nippon Kayaku Co. Ltd, 31-12, Shimo, 3-chome, Kita-ku 115-8588, Japan

Abstract

Background. Myeloperoxidase-specific anti-neutrophil cytoplasmic auto-antibody (MPO-ANCA) has been a useful diagnostic marker in systemic vasculitis with crescentic glomerulonephritis (CrGN). It is highly suspected that the antigenic enzyme MPO released from activated neutrophils is involved in these lesions. We evaluated the relationship between neutrophil functions including peripheral neutrophil counts and renal lesions in SCG/Kj mice as a model of ANCA-associated CrGN and vasculitis.

Methods. Peripheral neutrophil counts, the plasma levels of MPO-ANCA and tumour necrosis factor alpha (TNF-α) were measured. The capacity of MPO release and superoxide generation were evaluated as neutrophil activity. The renal lesions were estimated by grade of proteinuria, histopathological lesion, such as glomerular neutrophil infiltration and active or chronic renal injury scores with crescent formation.

Results. MPO-ANCA and TNF-α levels were higher than those of normal mice C57BL/6 even before overt proteinuria; subsequently, peripheral neutrophils increased. In the phase of nephritis with low grade proteinuria, the spontaneous release of MPO from peripheral neutrophils increased, while superoxide generation increased before spontaneous MPO release occurred. In addition, the renal lesion in histological observations was aggravated with ageing and the glomerular neutrophil infiltration was positively correlated with MPO-ANCA levels, as well as with histological indices of nephritis, active renal injury score; in particular, crescent formation was correlated with spontaneous MPO release. In contrast, superoxide generation was negatively correlated with the severity of this lesion during the progression.

Conclusions. These findings indicate that neutrophils are activated and contribute to the development of the active crescentic lesion in SCG/Kj mice.

Keywords: activated neutrophils; crescentic glomerulonephritis; MPO-ANCA; SCG/Kj mice; TNF-α

Introduction

In acute inflammatory disorders, multiple pathological processes are linked to the ability of neutrophils to release a complex assortment of agents that can destroy normal cells and dissolve connective tissue. As one of these agents, reactive oxygen intermediates (ROI) have been known to have a potential for tissue destruction [1]. In the presence of neutrophil-derived myeloperoxidase (MPO), even small amounts of ROI generate hypochlorus acid and then initiate the deactivation of antiproteases or activation of latent proteases, which lead to tissue damage if not properly controlled.

Antibodies directed against cytoplasmic constituents of the neutrophilic granulocyte have been extensively described as markers for systemic vasculitis and crescentic glomerulonephritis (CrGN) [2]. It has also been shown that MPO and the MPO-specific anti-neutrophil cytoplasmic auto-antibody (MPO-ANCA) are risk factors for the development of these lesions, possibly through ROI production as described above. In the sera of patients with microscopic polyangiitis [3] and CrGN [2], high titres of MPO-ANCA are frequently detected. Although it has been demonstrated

Correspondence and offprint requests to: Kazuo Suzuki, PhD, Chief of Biodefense Laboratory, National Institute of Infectious Diseases (NIID-NIH), Toyama 1-23-1, Shinjuku-ku, Tokyo, 162-8640, Japan. Email: ksuzuki@nih.go.jp. The authors wish it to be known that, in their opinion, the first two authors should be regarded as joint First Authors.

the role of neutrophil activation and MPO-ANCA as the initial risk of these lesions, it is necessary to investigate the precise network between neutrophils activation and development of CrGN.

As the basis for clinical studies, animal models are often used to understand the mechanisms of the development of vasculitis, and to establish therapeutic strategies. Both MRL lpr/lpr [4] and SCG/Kj [5] strains are known to show high levels of MPO-ANCA in association with renal lesions, including glomerulonephritis (GN) and vasculitis. Recently, using MPO KO mice we have clarified that MPO is a major antigen for MPO-ANCA production [6]. Moreover, the study using NZB/W F1 mice with the Fcg receptor deficiency has shown that the Fcg receptor on neutrophils and/or macrophages is necessary for the occurrence of GN [7]. Recently, using $Rag2^{-/-}$ and C57BL/6J mice, Xiao *et al.* [8] have demonstrated that anti-MPO IgG antibodies cause pauci-immune glomerular necrosis and crescent formation both in the presence or absence of functional T or B lymphocytes. Other studies have identified the gene responsible for GN and vasculitis [9]. However, the more precise pathogenic roles of MPO-ANCA and neutrophils in the development of GN and vasculitis in these murine models are undetermined.

In the present study, using SCG/Kj mice, a model of spontaneous CrGN and vasculitis, the role of activated neutrophils in the development of nephritis was investigated by evaluating the relationship between neutrophil function and renal lesions.

Subjects and methods

Mice

Female C57BL/6 mice were purchased from SLC Corporation (Shizuoka, Japan). Female SCG/Kj mice were bred and maintained at the animal facility of Nippon Kayaku Co. Ltd. Both mouse strains were maintained under specific pathogen-free conditions, and treated according to guidelines for animal care.

Reagents

fMet-Leu-Phe (FMLP) was purchased from Peptide Institute (Osaka, Japan). 3,3′, 5,5′-Tetramethylbendizine (TMB), cytochalasin B (CB), cytochrome *c* and phosphatase substrate were obtained from Sigma Chemical Company (St Louis, MO, USA). Alkaline phosphatase (AP)-labeled anti-mouse IgG was purchased from Cappel Corporation (West Chester, PA, USA), AP-labeled anti-human IgG antibody was purchased from Bio-Rad Corporation (Hercules, CA, USA). A kit for mouse TNF-α immunoassay was purchased from R & D Systems (Minneapolis, MN, USA). Nycoprep and 1 Step Polymorphs, for preparation of blood cells, were obtained from Nycomed Pharma AS (Oslo, Norway) and Chemical and Scientific Corporation (Osaka, Japan), respectively. Urine biochemical assay sticks were purchased from Bayel Medical Corporation (Tokyo, Japan). PQE-30, restriction enzymes and Ligation High were purchased from Qiagen (Hilden, Germany), TaKaRa (Shiga, Japan) and Toyobo (Osaka, Japan), respectively.

Grouping of SCG/Kj mice according to proteinuria

SCG/Kj mice were divided into three groups depending on the grades of proteinuria because proteinuria is one of the reliable indices of renal damage and the severity of GN in these mice did not always synchronize with age. Haematuria is often used as a marker of active CrGN in human cases, however, in the present study, proteinuria was employed as a marker of the severity of nephritis because the mice died at the onset of haematuria.

Proteinuria was determined by using a clinical stick as a marker for the onset and development of nephritis. In this study, the 'initial' phase was defined as below 30 mg/dl of proteinuria ($n=6$, age 8.2 ± 0.4 weeks), the 'early' phase of nephritis was defined as 30–300 mg/dl ($n=18$, age 12.7 ± 2.1 weeks) and the 'late' phase of nephritis was defined as over 300 mg/dl ($n=21$, age 13.1 ± 1.3 weeks), respectively. The damage to the renal lesion of the mice showed heterogeneity not dependent on their age. C57BL/6 mice of 9 and 14 weeks of age were used as normal mice.

Preparation of recombinant mouse MPO (rmMPO) and antibody to rmMPO

rmMPO was prepared by the expression in *Escherichia coli* transfected with a plasmid containing cDNA of mouse MPO. The cDNA pool was obtained from bone marrow cells of C57BL/6 mice by a PCR technique and ligated into an expression vector pQE-30. The mouse MPO cDNA was amplified by PCR from the cDNA pool using Platinum *Taq* DNA polymerase High Fidelity (Life Technologies, PTC-200; MJ Research, Waltham, MA, USA) using a ThermoScript RT-PCR System (Invitrogen Corp., Carlsbad, CA, USA). The MPO cDNA sequence we amplified was different from GenBank X15313 at 27 sites for six positions in the amino acid (Figure 1a). It was ligated in an expression vector pQE-30 between the BamHI site and the HindIII site. We transformed the plasmid into a host *E.coli* SG13009[pREP4] (Qiagen, Tokyo, Japan). The expressed protein consisted of His-tag-L-chain-H-chain of mouse MPO (Figure 1b). The bacteria were cultured in a medium containing Terrific Broth, 100 mg/ml ampicillin and 25 mg/ml kanamycin until ~4.6 of absorbance at 600 nm after addition of isopropyl-β-D-thiogalactopyranoside (IPTG), then we obtained with higher yield of rmMPO. The bacteria were lysed by sonication in 6 M guanidine-hydrogen chloride and then we purified the recombinant protein with affinity chromatography using a Ni-attached gel (Ni-NTA agarose; Qiagen) in 8 M urea, as described elsewhere [10] (Figure 1c). The IgG fraction of the polyclonal antibody to mouse MPO was prepared from serum of rabbit immunized with rmMPO and purified with Protein A (Pharmacia Fine Chemicals, Uppsala, Sweden) (Figure 1d). In addition, to evaluate the MPO-ANCA titre as equivalent to human MPO-ANCA, human MPO III was isolated from neutrophils of healthy volunteers, as previously described [11]. Briefly, neutrophils were extracted by detergents and purified by a series of DEAE and CM chromatography steps and HPLC. The completely purified sample had a Reinheitzahl (Rz) value, with an absorbance ratio of 430 to 280 nm of >0.7.

Measurement of MPO-ANCA levels in sera by ELISA

Sera were prepared from the abdominal aorta blood of the mice. MPO-ANCA levels were measured as described

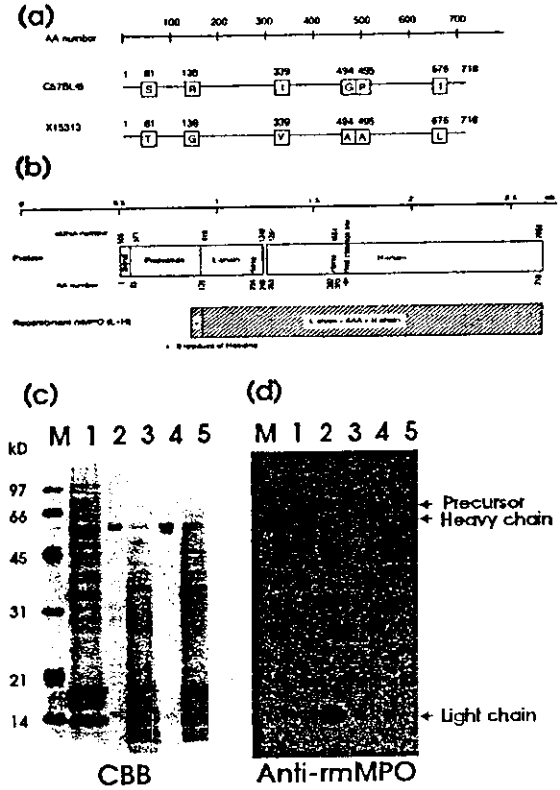

Fig. 1. Preparation of anti-rmMPO by rmMPO and evaluation of the antibody with western blotting. (a) Structure difference in mouse MPO between X15313 in GenBank and C57BL/6. (b) Construction of rmMPO. (c) Proteins in purification step. M, marker; 1, mouse neutrophils; 2, purified native mouse MPO; 3, human neutrophils; 4, purified human MPO; 5, human mononuclear cells; CBB, Coomassie brilliant blue stain.

previously [6]. Briefly, human MPO III was coated onto an ELISA plate (TS plate; Toyoshima Co., Tokyo, Japan) overnight at 4°C. The plate was blocked and mouse serum (×50 dilution) was added for 1.5 h at room temperature. AP-labeled anti-mouse IgG antibody (×1000 dilution) or an AP-labeled anti-human IgG antibody (×3000 dilution) was added and allowed to react for 2 h at room temperature. Afterwards, *p*-nitrophenylphosphate, an AP substrate, was added at a concentration of 1 mg/ml. After incubation at room temperature, the absorbance at 405 nm was measured by a model LFA-096 automatic analyser. The titre of MPO-ANCA in mouse sera was determined with human standard serum to obtain the human ELISA unit equivalent (hEU).

Measurement of TNF-μ in plasma

The diluted plasma (50 ml) was added to the each well of a 96 well F-plate and incubated for 2 h at room temperature. Each well was aspirated and washed five times; subsequently, 100 μl of conjugate was added to each well and incubated for 2 h at room temperature. This process was repeated with a 30 min incubation period upon addition of the substrate solution. Finally, 100 μl of stop solution was added to each well and absorbance measured at 450 nm.

Preparation of peripheral neutrophils of SCG/Kj mice

Heparinized blood, taken from the abdominal aorta of the mouse, was put onto the continuous preparation reagents, which consisted of 1.5 ml of Nycoprep, with a density of 1.077, added to 1.5 ml of 1 Step Polymorphs with a density of 1.113, and subsequently centrifuged for 30 min at 600*g* at 20°C. Neutrophils were obtained in the layer between the two reagents. Erythrocytes contained in the neutrophil fraction were lysed to obtain the neutrophils. Confirmation of over 85% yield of neutrophils was demonstrated by staining with a peroxidase detection kit (Muto Pure Chemicals Co., Ltd, Tokyo, Japan). Cell viability >99% was detected by trypan blue dye exclusion.

Measurement of MPO release and superoxide generation of neutrophils

Neutrophil degranulation, measurement of MPO release and superoxide generation were performed as described previously [12]. Briefly, neutrophils, which were pre-warmed for 10 min at 37°C, were stimulated in the presence or absence of CB and FMLP in a 96 well V-plate for 10 min at 37°C. After incubation, the plate was immersed in ice and then centrifuged at 350*g* for 5 min at 4°C to separate the supernatant from the cell pellet. MPO activity in the supernatant and cell lysate was assayed by the TMB method, as described previously [12]. Superoxide generation of neutrophils was determined by measuring the reduction of cytochrome *c*.

Histological examination of glomeruli

Haematoxylin–eosin and periodic acid-Schiff (PAS) staining. Kidneys were removed, fixed with buffered formalin, and embedded in paraffin. To assess the activity and chronicity of the lesions in SCG/Kj mice, serial 4 μm sections were stained with haematoxylin–eosin and periodic acid-Schiff.

Immunoperoxidase staining for neutrophils. Neutrophils were confirmed by an indirect method using a polyclonal rabbit antibody against rmMPO as described previously [13]. Briefly, the sections were incubated with the primary antibody followed by biotinylated anti-rabbit IgG (Vector Laboratories, Burlingame, CA, USA). The sections were then reacted with avidin-DH-biotinylated horseradish peroxidase complex (Vectastain ABC kit; Vector Laboratories). Colour was then developed by incubation with an ImmunoPure Metal Enhanced DAB Substrate kit (Pierce, Rockford, IL, USA).

Evaluation of renal lesion. The number of the infiltrated neutrophils into 20 glomeruli was counted based on nuclear morphology of HE and PAS staining. Matrix expansion was also measured. Moreover, each specimen was used to determine the activity index (AI) and chronicity index (CI) according to the modified NIH criteria by Austin *et al.* [14], originally developed for systemic lupus erythematosus, as follows. The AI was scored in the presence of cell proliferation, cellular and fibrocellular crescent formation, interstitial

mononuclear cell infiltration, and small vessel vasculitis. The presence of cell proliferation and interstitial mononuclear cell infiltration was scored in a range of 0–3 (0 = absent, 1 = mild, 2 = moderate and 3 = severe). The presence of cellular or fibrocellular crescents was scored in a range of 0–3 (0 = absent, 1 = <20% of the glomeruli involved, 2 = 20–50% glomeruli involved, 3 = >50% glomeruli involved). The maximal activity score amounted to 10. The CI scored the presence of matrix expansion (0–3), global glomerulosclerosis (0–3), and tubulointerstitial change such as tubular atrophy and/or interstitial fibrosis (0–3). The maximal chronicity index amounted to 12. The crescent score was evaluated by the modified method of Floege [15] as follows: 40 glomerular cross-sections were graded by a relative area of the cellular crescent occupied in Bowman's capsule as 0, negative; 1, 1–25%; 2, 26–50%; 3, 51–75%; 4, 76–100%; and then the total grade in 40 glomeruli was defined as the crescent score.

Statistical analysis

Values were expressed as mean ± SD and were analysed for statistical differences by the Mann–Whitney *U*-test. Correlations were analysed by the Pearson test. The probability value of <0.05 was considered significant.

Results

The changes of neutrophil counts, MPO-ANCA levels and TNF-α in peripheral blood related with the nephritis development

The peripheral neutrophil count did not increase in C57BL/6 mice with ageing. In SCG/Kj mice, the count was significantly elevated in the early phase. It also increased in the late phase. As a result, peripheral neutrophil counts in both early and late phases significantly increased compared with those of control C57BL/6 mice and in the initial phase of SCG/Kj mice (Figure 2a).

The serum levels of MPO-ANCA in SCG/Kj mice in all phases of nephritis were higher than those in C57BL/6 mice (Figure 2b). Ratios of SCG/Kj mice showing MPO-ANCA positive in sera were 17.6% in the initial phase, 11.1% in the early phase and 20% in the late phase, respectively. Two mice showed positive values of MPO-ANCA without crescent formation (data not shown).

Plasma TNF-α levels of SCG/Kj mice were significantly higher than those in C57BL/6 mice, particularly in the early phase. The increase was significant, compared either with control mice or with the initial phase of nephritis in SCG/Kj mice (Figure 2c).

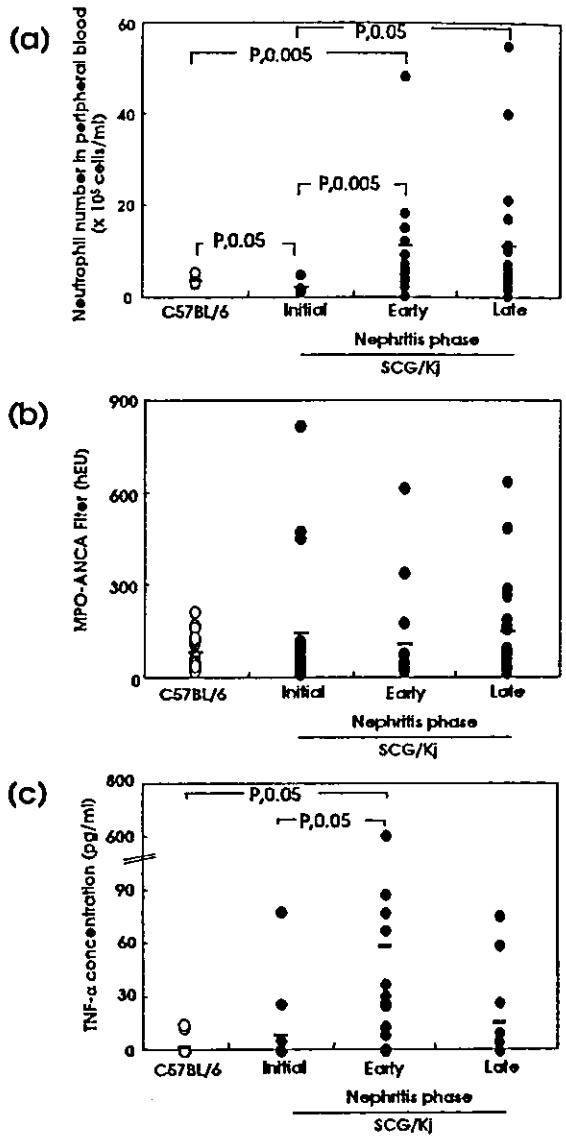

Fig. 2. Peripheral neutrophil counts and MPO-ANCA levels in the sera and plasma TNF-α concentrations in SCG/Kj mice. (a) Peripheral neutrophil counts. (b) MPO-ANCA levels in the sera. (c) TNF-α concentration in the plasma in SCG/Kj and C57BL/6 mice. The initial phase of nephritis: <30 mg/dl of proteinuria; the early phase of nephritis: 30–300 mg/dl of proteinuria; the late phase of nephritis: >300 mg/dl of proteinuria.

Neutrophil function in each phase of nephritis

Spontaneous and FMLP stimulated MPO release from peripheral neutrophil. In SCG/Kj mice, although spontaneous MPO release from peripheral neutrophils was relatively enhanced in the early phase of nephritis (Figure 3a), there was no marked difference in the levels. FMLP-induced MPO release showed no difference in all phases and between two strains of mice (Figure 3b).

Superoxide generation from peripheral neutrophils. Superoxide generation in SCG/Kj mice was higher than that of control mice. In particular, it was significantly enhanced in the initial phase of nephritis (Figure 3c).

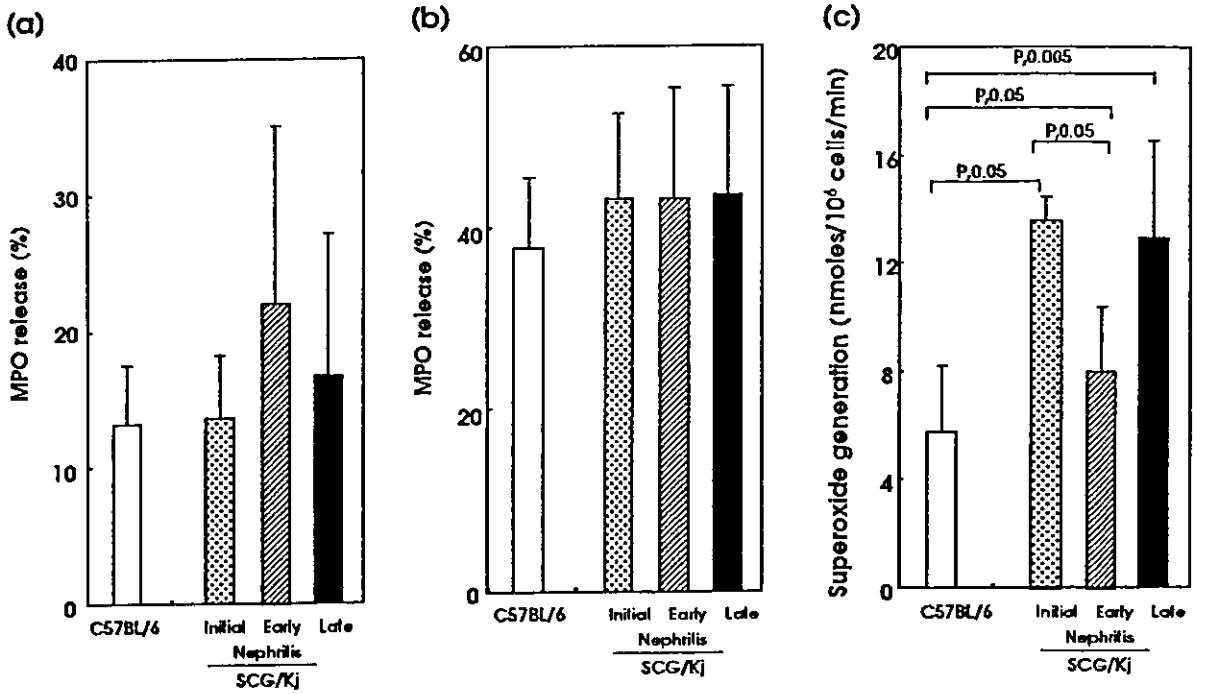

Fig. 3. Neutrophil activation in SCG/Kj mice. MPO release from neutrophils in SCG/Kj mice. Prewarmed neutrophils (10^6 cells/ml) were stimulated (a) in the absence or (b) presence of FMLP (10^{-5} M) and CB (5 μg/ml). (c) Superoxide generation in SCG/Kj and C57BL/6 mice.

Table 1. Renal lesion of SCG/Kj mice with ageing.

Age range (weeks)	Activity Index	Chronicity Index	Crescent formation (%)	Neutrophil infiltration (glomerulus)	Matrix expansion
8–9 (mean 8.17±0.41)	2.33±0.82	1.00±0	0.55±0.63	0.44±0.11	1.00±0
10–12 (mean 11.31±0.63)	3.77±1.09	2.15±0.38*	0.8±1.06	0.84±0.42	2.15±0.38*
13–16 (mean 13.96±0.89)	4.92±1.73*	2.64±1.32*	10.96±18.00	1.10±0.57*	2.08±0.49*

*$P<0.05$

Renal lesion with ageing in histological findings of SCG/Kj mice

The changes of characteristics of renal lesion with ageing in SCG/Kj mice are shown in Table 1. Both AI and CI significantly increased depending on age (Table 1). Crescent formation markedly increased after ageing, although there was no statistical significance among ages. Any interstitial fibrosis was not detected but some global sclerosis was also detected in these mice (data not shown). Vasculitis was detected in two mice irrespective of age at 10 and 14 weeks (data not shown). Glomerular neutrophil infiltration significantly increased with the development after 13 weeks of age (Table 1). In severe nephritis with cellular crescent formation, marked infiltration was often observed in the glomeruli (Figure 4a). We confirmed neutrophils by staining with antibody against MPO (Figure 4b). Although matrix expansion significantly increased from 10 weeks of age, these increases did not enhance with ageing (Table 1).

Relationship between glomerular neutrophil infiltration and parameters of histological findings in SCG/Kj mice

Glomerular neutrophil infiltration correlated with the AI (Figure 5a), with the crescent formation score (Figure 5b) and with the CI ($R=0.43$, $P<0.01$, data not shown). In addition, it correlated with MPO-ANCA levels in sera (Figure 5c), although there was no direct relationship between serum levels of MPO-ANCA and crescent formation score.

Relationship between neutrophil function and histological lesions

We analysed the influence of neutrophil activity measured by spontaneous MPO release in the histological lesions in SCG/Kj mice. Spontaneous MPO release was positively correlated with not only crescent formation score (Figure 6a), but also the renal AI (Figure 6b) (crescent formation score, $R=0.39$, $P<0.05$; AI, $R=0.32$, $P<0.05$). This correlation was

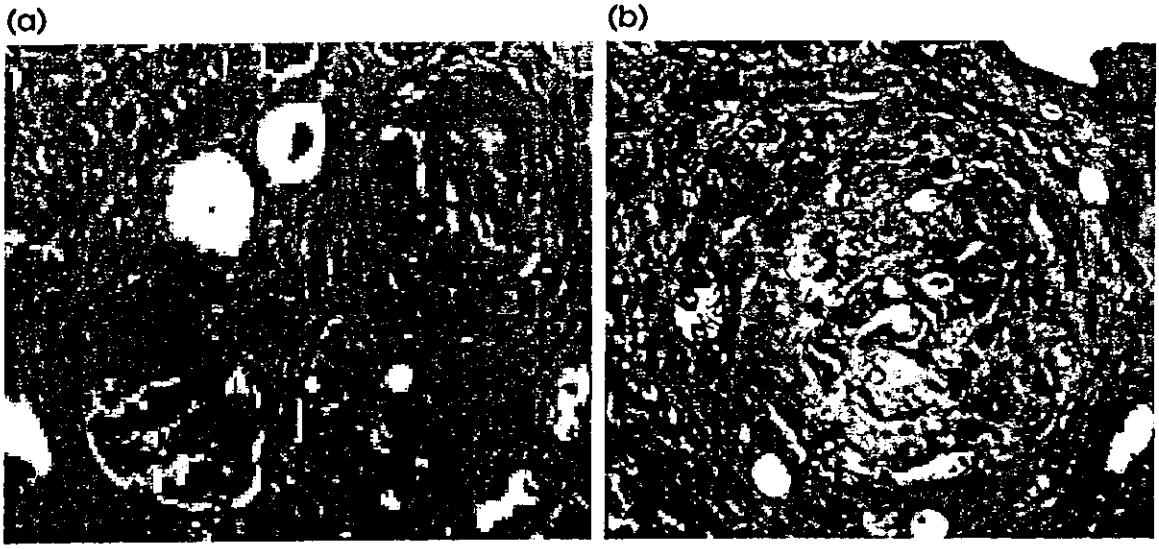

Fig. 4. Renal histological analysis in SCG/Kj mice. Correlation between neutrophil infiltration into the glomeruli and renal injury. (a) Light microscopy of infiltrated neutrophils into the glomeruli in the late phase of nephritis. Periodic acid-Schiff staining were performed (final magnification ×200). (b) Neutrophils, which were positive for rmMPO staining, were abundantly observed in the tissue from the late phase of nephritis (final magnification ×400).

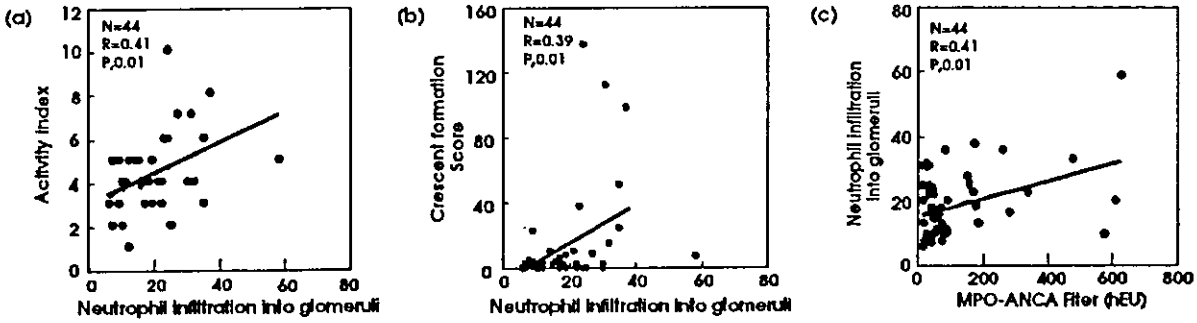

Fig. 5. Correlation between neutrophil infiltration into the glomeruli and renal injury in SCG/Kj mice. (a) Correlation between neutrophil infiltration into the glomeruli and AI ($n=44$, $R=0.41$, $P<0.01$). (b) Correlation between neutrophil infiltration into the glomeruli and the crescent formation score ($n=44$, $R=0.39$, $P<0.01$). (c) Correlation between neutrophil infiltration into the glomeruli and MPO-ANCA levels ($n=44$, $R=0.41$, $P<0.01$).

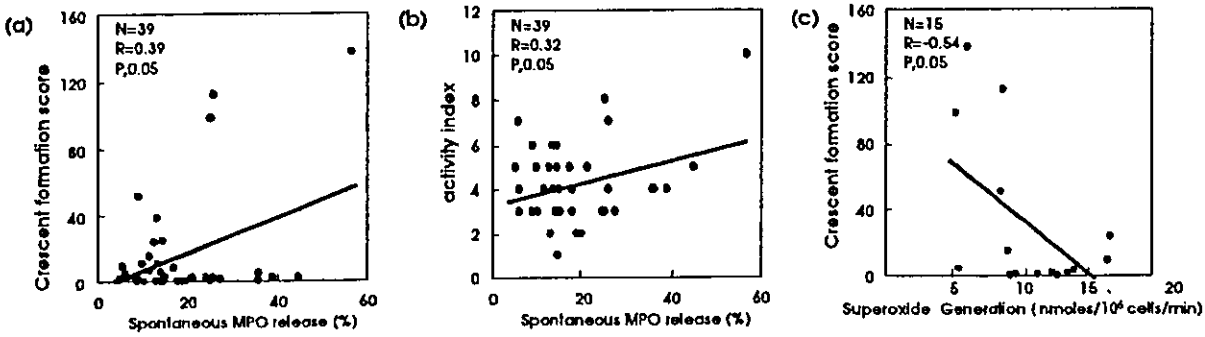

Fig. 6. Correlation between neutrophil activation and renal injury in SCG/Kj mice. (a) Correlation between spontaneous MPO release and crescent formation score AI in the early phase ($n=39$, $R=0.39$, $P<0.05$). (b) Correlation between spontaneous MPO release and AI ($n=39$, $R=0.32$, $P<0.05$). (c) Negative correlation between superoxide generation and the crescent formation score ($n=15$, $R=-0.54$, $P<0.05$)

also obtained with the renal CI ($R=0.32$, $P<0.05$, data not shown). On the other hand, a negative correlation was noted between superoxide generation and crescent formation score (Figure 6c).

Discussion

Rapidly progressive glomerulonephritis (RPGN) is a severe form of immune-mediated renal disease that is often poorly responsive to therapy [16]. SCG/Kj mice have been reported as a potent animal model for human RPGN [5,17,18]. In the original report, 58% of female mice revealed RPGN [17]. As shown in our study, marked crescent formation was detected in their renal tissue associated with a variety of proteinuria from a relatively early age.

In the present study, we examined the contribution of activated neutrophils to the development of nephritis in this strain of mice. As the development of renal lesions showed marked heterogeneity, independent of age, we classified its severity of nephritis into three phases (initial, early and late phases) depending on the grade of proteinuria.

The number of mice with a high peripheral neutrophil count increased along with the severity of nephritis. In all phases of nephritis, MPO-ANCA levels in sera were higher in SCG/Kj mice than those in control mice, although a statistical difference could not be obtained. These observations in mice are similar to that of the patient with RPGN.

TNF-α levels in plasma significantly increased in the early phase of nephritis in SCG/Kj mice. Dewas *et al.* [19] have recently reported that TNF-α, via its p55 receptor, induces protein tyrosine kinase-dependent selective phosphorylation of $p47^{phox}$ on specific serines in human neutrophils. On the other hand, Timoshanko *et al.* [20] have reported that intrinsic renal cells are the major cellular source of TNF-α contributing to inflammatory injury in CrGN. These findings suggest that neutrophils primed with TNF-α produce superoxide through activation of NADPH oxidase. Based on our data, elevation of superoxide generation in the initial phase was coincident with higher levels of TNF-α in the plasma. These observations suggest that in the initial phase of CrGN, peripheral neutrophils may be activated with TNF-α priming. Subsequently, activated neutrophils showed a release of MPO without stimulation in the early phase, but superoxide generation was already activated in the initial phase, suggesting that activated neutrophils are easy to degranulation with no stimulation. In addition, decrease of superoxide generation in the early phase may be a result of suppression of the cascade of NADPH oxidase activation, which occurs due to desensitization of neutrophils after the initial phase. Higher counts of activated neutrophils in peripheral blood from early phase to late phase may cause damage to endothelial cells, resulting in the vascular lesion involved in CrGN. Indeed, spontaneous MPO release from peripheral neutrophils was correlated with the crescent formation score, AI and CI, but negative correlation in superoxide generation, suggesting activated neutrophils cause the renal lesion.

A correlation between glomerular neutrophil infiltration and increased MPO-ANCA levels was shown in SCG/Kj mice. This reflects the correlation between neutrophil activation and increased MPO-ANCA levels in the sera of patients with GN. Bajema *et al.* [21] reported co-localization of MPO and fibrinoid necrosis by using their double staining technique in ANCA-associated vasculitis. They have demonstrated that both neutrophils and liberated MPO exist in injured glomeruli tissue, suggesting that MPO may cause tissue damage by generating hypochlorous acid.

In addition, glomerular neutrophil infiltration was correlated with the crescent formation score, AI and CI. Miyazawa *et al.* [18] recently reported the important role of glomerular neutrophil influx as an initial response in the process of crescent formation in SCG/Kj mice. From these findings, neutrophil infiltration into glomeruli and MPO-ANCA production could be associated with the beginning of the renal lesion. On the other hand, MPO-ANCA production might be enhanced by the impaired clearance by apoptosis of activated or abnormal neutrophils, with or without other stimuli [22]. An increase of peripheral neutrophils escaping from apoptosis might directly injure renal tissue. Based on our data, MPO-ANCA production increased in the initial phase before elevation of proteinuria, suggesting that MPO-ANCA is a trigger for elevation of renal lesion. However, deposition of IgGs and complement 3 along peripheral capillary loops [5] and auto-antibodies against DNA and the glomerular basement membrane that are produced as a result of polyclonal B cell activation [4], could participate in pathogenesis of GN.

Neutrophils activated with TNF-α and MPO-ANCA may participate in the onset of CrGN by superoxide generation. Subsequently, degranulation, including MPO release, continuously damages the endothelium. Finally, constitutive neutrophil activation could be involved in active crescentic lesion of glomeruli in SCG/Kj mouse.

Acknowledgements. We thank Drs David Jayne, Consultant in Nephrology and Vasculitis, Addenbrookes Hospital, Cambridge, UK, Masahisa Kyogoku, Tohoku University School of Medicine, Sendai, Japan, Wayne K. Dawson and Amanda Persad, in NIID, Tokyo, Japan for their critical review of the manuscript. This work was supported in part by a grant for Researches of Measures for Intractable Diseases, Pharmaceutical and Medical Safety and Health Sciences focusing on Drug Innovation of Health and Labour Sciences Research Grants of Ministry of Health, Labour and Welfare.

Conflict of interest statement. None declared.

References

1. Johnson RJ, Couser WG, Chi EY *et al.* New mechanism for glomerular injury. Myeloperoxidase-hydrogen peroxide-halide system. *J Clin Invest* 1987; 79: 1379–1387

2. Arimura Y, Minoshima S, Kamiya Y *et al.* Serum myeloperoxidase and serum cytokines in anti-myeloperoxidase antibody-associated glomerulonephritis. *Clin Nephrol* 1993; 40: 256–264
3. Falk RJ, Nachman PH, Hogan SL *et al.* ANCA glomerulonephritis and vasculitis: a Chapel Hill perspective. *Semin Nephrol* 2000; 20: 233–243
4. Harper JM, Thiru S, Lockwood CM *et al.* Myeloperoxidase autoantibodies distinguish vasculitis mediated by anti-neutrophil cytoplasm antibodies from immune complex disease in MRL/Mp-lpr/lpr mice: a spontaneous model for human microscopic angiitis. *Eur J Immunol* 1998; 28: 2217–2226
5. Neumann I, Birck R, Newman M *et al.* SCG/Kinjoh mice: a model of ANCA-associated crescentic glomerulonephritis with immune deposits. *Kidney Int* 2003; 64: 140–148
6. Ishida-Okawara A, Oharaseki T, Takahashi K *et al.* Contribution of myeloperoxidase to coronary artery vasculitis associated with MPO-ANCA production. *Inflammation* 2001; 25: 381–387
7. Wakayama H, Hasegawa Y, Kawabe T *et al.* Abolition of anti-glomerular basement membrane antibody-mediated glomerulonephritis in FcRgamma-deficient mice. *Eur J Immunol* 2000; 30: 1182–1190
8. Xiao H, Heeringa P, Hu P *et al.* Antineutrophil cytoplasmic autoantibodies specific for myeloperoxidase cause glomerulonephritis and vasculitis in mice. *J Clin Invest* 2002; 110: 955–963
9. Wang Y, Nose M, Kamoto T *et al.* Host modifier genes affect mouse autoimmunity induced by the lpr gene. *Am J Pathol* 1997; 151: 1791–1798
10. Tomizawa K, Mine E, Fujii A *et al.* A panel set for epitope analysis of myeloperoxidase (MPO)-specific anti-neutrophil cytoplasmic antibody MPO-CA using recombinant hexamer histidine-tagged MPO deletion mutants. *J Clin Immunol* 1998; 18: 142–152
11. Suzuki K, Yamada M, Akashi K *et al.* Similarity of kinetics of three types of myeloperoxidase from human leukocytes and four types from HL-60 cells. *Arch Biochem Biophys* 1986; 245: 167–173
12. Ishida-Okawara A, Kimoto Y, Watanabe K *et al.* Purification and characterization of aseanostatins: actinomycete-derived fatty acid inhibitors to myeloperoxidase release from human polymorphonuclear leukocytes. *J Antibiot* 1991; 44: 524–532
13. Liu N, Ono T, Suyama K *et al.* Factor V expression colocalized with fibrin deposition in IgA nephropathy *Kidney Int* 2000; 58: 598–606
14. Austin HA 3rd, Muenz LR, Joyce KM *et al.* Prognostic factors in lupus nephritis. Contribution of renal histologic data. *Am J Med* 1983; 75: 382–391
15. Floege J, Johnson RJ, Gordon K. *et al.* Increased synthesis of extracellular matrix in mesangial proliferative nephritis. *Kidney Int* 1991; 40: 477–478
16. Zauner I, Bach D, Braun N *et al.* Predictive value of initial histology and effect of plasmapheresis on long-term prognosis of rapidly progressive glomerulonephritis. *Am J Kidney Dis* 2002; 39: 28–35
17. Kinjoh K, Kyogoku M, Good RA. Genetic selection for crescent formation yields mouse strain with rapidly progressive glomerulonephritis and small vessel vasculitis. *Proc Natl Acad Sci USA* 1993; 90: 3413–3417
18. Miyazawa S, Saiga K, Nemoto K *et al.* A repeat biopsy study in spontaneous crescentic glomerulonephritis mice. *Ren Fail* 2002; 24: 557–566
19. Dewas C, Dang PM, Gougerot-Pocidalo MA *et al.* TNF-alpha induces phosphorylation of $p47^{phox}$ in human neutrophils: partial phosphorylation of $p47^{phox}$ is a common event of priming of human neutrophils by TNF-alpha and granulocyte-macrophage colony-stimulating factor. *J Immunol* 2003; 171: 4392–4398
20. Timoshanko JR, Sedgwick JD, Holdsworth SR *et al.* Intrinsic renal cells are the major source of tumor necrosis factor contributing to renal injury in murine crescentic glomerulonephritis. *J Am Soc Nephrol* 2003; 14: 1785–1793
21. Bajema IM, Hagen EC, de Heer E *et al.* Colocalization of ANCA-antigens and fibrinoid necrosis in ANCA-associated vasculitis. *Kidney Int* 2001; 60: 2025–2030
22. Potter PK, Cortes-Hernandez J, Quartier P *et al.* Lupus-prone mice have an abnormal response to thioglycolate and an impaired clearance of apoptotic cells. *J Immunol* 2003; 170: 3223–3232

Received for publication: 10.6.03
Accepted in revised form: 14.1.04

Available online at www.sciencedirect.com
SCIENCE DIRECT®
Gene 327 (2004) 195–200
GENE
AN INTERNATIONAL JOURNAL ON GENES AND GENOMES
www.elsevier.com/locate/gene

Novel missense mutation found in a Japanese patient with myeloperoxidase deficiency

Yuko Y. Ohashi[a], Yosuke Kameoka[b], Amanda S. Persad[a], Fumikazu Koi[c], Satoshi Yamagoe[a], Katsuyuki Hashimoto[b], Kazuo Suzuki[a,*]

[a] *Department of Bioactive Molecules, National Institute of Infectious Diseases, 1-23-1 Toyama, Shinjuku, Tokyo 162-8640, Japan*
[b] *Division of Genetic Resources, National Institute of Infectious Diseases, 1-23-1 Toyama, Shinjuku, Tokyo 162-8640, Japan*
[c] *Takamatsu Kyosai Hospital, 4-18 Tenjinmae, Takamatsu City 760-0081, Japan*

Received 23 July 2003; received in revised form 5 November 2003; accepted 14 November 2003

Abstract

Myeloperoxidase (MPO; EC 1.11.1.7) plays an important role in the host defense mechanism against microbial diseases. The neutrophil disorder characterized by the lack of MPO activity, is speculated to be associated with a decreased level of immunity. A Japanese patient was identified with complete MPO deficiency through automated hematography. Neutrophil function analysis revealed that MPO activity was significantly diminished with slightly elevated superoxide production. Mutational analysis of the patient revealed a glycine to serine substitution (G501S) in the exon 9 region. This mutation was not detected in the 96 healthy controls analyzed. The amino acid substitution found may be responsible for the failure of mature MPO production in the patient. This is the first case of MPO deficiency of G501S missense mutation identified in a Japanese patient.

Keywords: Myeloperoxidase; Deficiency; Neutrophills; Mutation heme-binding

1. Introduction

Myeloperoxidase (MPO) is a lysosomal heme protein located in azurophilic granules of neutrophils cells and monocytes. MPO is part of the host defense system and is responsible for microbicidal activity against a wide range of organisms. In activated neutrophils, MPO catalyzes the production of hypohalous acids, primarily hypochlorous acid and other toxic intermediates that greatly enhance neutrophil microbicidal activity. A deficiency in this enzyme (Mendelian inheritance in man (MIM) no. 254600) is considered to be responsible for weakening host defense activity against microbial diseases (Lanza, 1998). The prevalence of complete MPO deficiency in Japan is estimated to be 1.75/100,000, a value 14- to 28-fold lower than that of the United States and Europe, respectively (Suzuki et al., 2000; Nunoi et al., 2003). Aratani et al. (1999, 2000) has described the association with this deficiency and continuous infection of *Candida albicans* in MPO knock-out mice.

Three allelic mutations related to MPO deficiency have been previously reported: R569W (Nauseef et al., 1994, 1996), Y173C (DeLeo et al., 1998) and M251T (Romano et al., 1997). The defect mechanisms and manner of inheritance has been studied in detail (Nauseef et al., 1996, 1998). The enzyme deficiency is due to incapability to undergo posttranslational processing. Cases with alternative splicing and deletions have also been reported (Romano et al., 1997; Hashinaka et al., 1988).The biosynthesis of MPO includes N-linked glycosylation, heme insertion, proteolytic processing and dimerization (Gullberg et al., 1997). The R569W mutation results in an alteration in the normal translation and produces an enzymatically inactive, heme-free precursor apoproMPO (Nauseef et al., 1996). The Y173C mutation replaces the tyrosine at position 7 in the light subunit

Abbreviations: MPO, myeloperoxidase; BGL, beta-glucuronidase; HBSS, Hanks' balance salt solution; PVDF, polyvinylidene diflouride; AP, alkaline phosphatase; cDNA, DNA complementary to RNA; PCR, polymerase chain reaction; RT, reverse transcriptase; mRNA, messenger RNA; RT–PCR, polymerase chain reaction subsequent to reverse transcription.

* Corresponding author. Tel.: +81-3-5285-1111x2329; fax: +81-3-5285-1160.
E-mail address: ksuzuki@nih.go.jp (K. Suzuki).

0378-1119/$ - see front matter © 2004 Elsevier B.V. All rights reserved.
doi:10.1016/j.gene.2003.11.023

with a cysteine. Therefore, the potential for additional intramolecular disulfide bond would be created. Y173C mutation results in proMPO, however, it fails to mature into the enzymatically active MPO (DeLeo et al., 1998). The M251T mutation results in azurophilic granules, containing MPO that lacks enzyme activity (Romano et al., 1997).

We have found a patient of complete MPO deficiency in Japan. So far, no MPO mutational study among Japanese patients has been reported. In order to elucidate the background of the deficiency, we performed assays for enzyme activity and neutrophil chemotaxis, as well as mutational analysis of the patient and his mother.

2. Materials and methods

2.1. Subjects

A 39-year-old Japanese male was diagnosed with complete MPO deficiency by Bayer-Technicon automated hematography (Suzuki et al., 2000). Automated hematography is routinely used in the hospital system to further analyze unusual neutrophil activity. Informed consent was obtained from the patient and his mother (60 years old) for this study. The patient exhibited signs of obstructive pulmonary disease, although no history of recurrent infections or medication known to interfere with MPO activity were present or used. A blood sample from one healthy control was drawn to measure enzyme activity and superoxide production, however, controls for genetic sequencing consisted of DNA samples from 98 healthy donors of which MPO activity and superoxide activity could not be elucidated. Since MPO deficiency (both complete and partial deficiency) is very rare in Japan, less than 6 cases per 100,000 individuals, it is highly unlikely that these 98 healthy donors were deficient in this enzyme (Suzuki et al., 2000; Nunoi et al., 2003).

2.2. Assay of MPO release from neutrophils

MPO release from neutrophils was assayed as described previously (Kawai et al., 2000). Neutrophils (10^6 cells/ml in Hanks' balance salt solution, HBSS) were prewarmed for 10 min at 37 °C and transferred into a 96-well V-plate containing cytochalasin B (CB; 5 μg/ml) (Sigma-Aldrich Japan, Tokyo) and fMet–Leu–Phe (FMLP, 10^{-5} M) (Protein Research Foundation, Osaka) in a total volume of 75 μl. After incubation for 10 min at 37 °C, cell suspensions were centrifuged at $400 \times g$ for 5 min. MPO activity in the supernatant and in the homogenate of the cell pellet was measured spectrophotometrically using 3,3′, 5,5′-tetramethylbenzidine as substrate (Suzuki et al., 1983, 1986). The total enzyme activity of MPO in neutrophils was calculated as the sum of enzyme activity in supernatants and homogenate after treatment with CB and FMLP. Release of MPO was expressed as percentage of total enzyme activity (MPO activity in supernatant/total enzyme activity).

2.3. Measurement of beta-glucuronidase (BGL) activity

Beta-glucuronidase activity and release was elicited by methods described previously (Minoshima et al., 1997). Cell supernatant and homogenate (40 μl) was treated with 1 mmol/l 4-methylumbelliferyl-beta-D-glucuronide, 0.05% Triton X-100 and 0.1 mol/l sodium acetate buffer (pH 3.5) in 96-well flat bottom plate. After 30 min of incubation at 37 °C, the reaction was stopped by adding 210 μl of termination buffer (50 mmol/l sodium glycine buffer pH 10.4 supplemented with 5 mmol/l EDTA). Fluorescence intensity was measured by using an automated fluorescence analyzer LFA-096F (Japan Spectroscopic, Tokyo, Japan). One unit of BGL activity was defined as the activity of 1 pmol of 4-methylumbelliferon/min per milliliter of the original enzyme preparation.

2.4. Determination of O_2^- production by neutrophils

Superoxide (O_2^-) production by neutrophils was determined using methods previously described (Kawai et al., 2000). Briefly, neutrophil suspensions (2.0×10^6 cells/ml, 100 μl) and 66 μM of ferricytochrome *c* (Sigma-Aldrich Japan) were mixed in a 96-well F-plate and held at 37 °C for approximately 2 min. CB (5 μg/ml) and FMLP (10^{-5} M) were added to the suspension and incubated for approximately 30 s at 37 °C. An initial velocity of O_2^- production was determined by measuring the increase in absorbance at 550 nm at 1.0-min intervals using a microplate reader.

2.5. Western blot analysis

Immunoblotting of neutrophils from patient, his mother and healthy control was performed as follows. The neutrophils (2×10^6 cells/200 μl) and purified MPO (100 ng/10 μl) were dissolved in loading buffer (50 mM Tris–HCl pH6.8, 10% glycerol, 1% SDS, 0.3 M beta-mercaptoethanol, 0.01% BPB) and incubate for 5 min at 98 °C to ensure completed reduction conditions, then quickly chilled on ice. Ten milliliters of each sample was fractionated on an 8–12% SDS–polyacrylamide gel according to Laemmli's system (Laemmli, 1970) and electrically transferred on to a polyvinylidene diflouride (PVDF) membrane (Millipore, Bedford, MA) in transfer buffer (20% methanol, 25 mmol/l Tris, 0.19 mol/l glycine). Membrane was incubated with a 1:2000 anti-human MPO rabbit antibody (Dako, Glostrup, Denmark) at room temperature for 2 h, followed by an incubation with a 1:2000 alkaline phosphatase (AP)-conjugated anti-rabbit IgG goat antibody (Organon Teknika, Durham, NC) for 2 h. Finally, the membrane was visualized using AP conjugate substrate kit (Bio-Rad, Hercules, CA, USA).

2.6. cDNA and genomic DNA analysis

MPO cDNA was acquired from the mRNA of mononuclear cells (MNC) by polymerase chain reaction (PCR)

Table 1
PCR primers used to detect (a) mRNA and (b) genomic sequence of MPO

DNA fragment	F/R	Position	Sequence (5′–3′)
(a) mRNA			
Fragment 1	F	−148	ccttggaagctggatgacagcagct
	R	+346	gctgactacctgcacgtggct
Fragment 2	F	+295	ctatcctacttcaagcagccg
	R	+741	cgctcactcatgttcatgcaa
Fragment 3	F	+694	aacgagatcgtgcgcttcccc
	R	+1123	ggcctgctgccctttgacaac
Fragment 4	F	+1063	aacatgtccaaccagctgggg
	R	+1530	aatcggtaccagcccatggaa
Fragment 5	F	+1498	tacggccacaccctcatccaa
	R	+1960	aaaggccgcgtgggcccactc
Fragment 6	F	+1918	atcgacatctggatgggcggc
	R	+2406	ggcttttcatgcgtgaaaaaaa
(b) Genomic fragment			
5′-flanking	F	−556	ctgagaaatcttgggctggtagtgct
	R	+36	tccttggaagctggatgacagcagct
Exon 1	F	−66	agaggacataaaagcgcag
	R	+302	aaggtgggagaagatggtgt
Exon 9	F	+7195	agatacttcccctgacctgg
	R	+7495	gacctaggccagagcgagtg

Primers were designed from the published sequence (Genbank accession nos. X04876 and X15377).
F = forward primer; R = reverse primer. Positons of primer are indicated by base number from the adenine of the first ATG.

using the One Step RNA PCR Kit (Takara, Kyoto, Japan). The specific primer pairs for MPO mRNA are shown in Table 1. DNA segments obtained were purified by the QIAquick PCR purification system (Qiagen, Hilden, Germany) and subjected to direct sequencing as described by the manufacturer. Purified fragments served as templates in a PRISM Ready Reaction Dye Terminator Cycle Sequencing procedure utilizing a 310 automatic sequencer (Applied Biosystems, Foster City, CA, USA). Primers used for sequencing are listed in Table 1. Additionally, the prevalence of −463 G/A polymorphism, a previously described mutation found in the promoter region of MPO (Reynolds et al., 2002), among controls was ascertained.

3. Results

3.1. Neutrophil functions and MPO activity

Total MPO activity of the patient was 250-fold lower than the healthy control, while the mother had half the activity of the control (Table 2). FMLP and cytochalasin B-induced MPO release was not detected in the patient, while the released MPO activity of the mother and the healthy control showed no marked difference. To examine the normal formation of azurophil granules, in which MPO is enclosed, BGL release and O_2^- production were assayed. BGL release was elicited by methods described previously (Minoshima et al., 1997). The patient, patient's mother and healthy control showed no difference in BGL and O_2^- production.

Table 2
Enzyme activities and functions of polymorphonuclear cells

	MPO		BGL		O_2^- production (nmol/min/10^6 cells)
	Total activity unit	% Release	Total activity unit	% Release	
Patient	0.3	N.D.	570	55.2	18
Mother	30.5	33.5	651	24.1	10.9
Healthy control	75.7*	22.9	430	32.7	14.1

N.D. = not detected; N.T. = not tested.
* Average in two experiments.

Azurophil granule formation under histochemical observation and O_2^- production of the patient showed no substantial difference from healthy control. Neutrophils may have developed normally but lack only mature MPO protein. As the mother showed half the MPO activity of the healthy control, there might be a quantitative effect of an abnormal allele in the mother.

3.2. Western blot analysis

In order to biochemically characterized MPO, immunoblotting analysis of the neutrophils from the healthy control, the patient, his mother and purified MPO were performed using anti-human MPO antibody. As shown in Fig. 1, the 59-kDa mature heavy subunit and the 14-kDa light subunit could not be detected in the patient, while the healthy control and mother had both mature subunits.

3.3. Mutational analysis

MPO cDNA, acquired by reverse transcription (RT)–PCR, were found to be the appropriate length in for each fragment amplified. Therefore, MPO gene in the patient was normally transcribed without any alternative transcription.

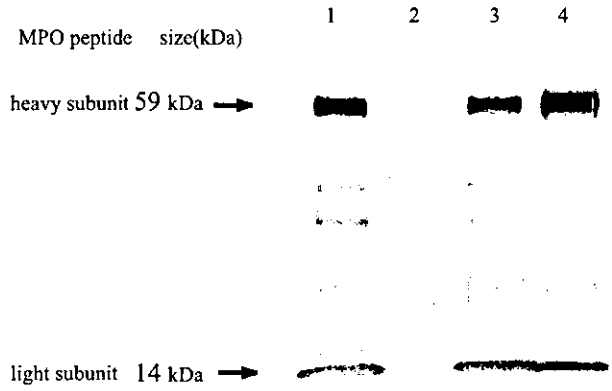

Fig. 1. Western blot analysis. Proteins in neutrophils (1×10^5 cells/lane) of healthy control, the patient, his mother and purified MPO protein (100 ng/lane) was fractionated on 8–12% polyacrylamide gel, transferred on PVDF membrane, and detected by rabbit anti-human MPO antibody. Lane 1, healthy control; lane 2, patient; lane 3, mother; and lane 4, purified human MPO. MPO polypeptides were indicated in the left.